May 2017

On Some One-Complex Dimensional Slices of the Boundedness Locus of a Multi-Parameter Rational Family

Matthew Hoeppner
University of Wisconsin-Milwaukee

ON SOME ONE-COMPLEX DIMENSIONAL SLICES OF THE BOUNDEDNESS LOCUS OF A MULTI-PARAMETER RATIONAL FAMILY

by

Matthew Hoeppner

A Dissertation Submitted in

Partial Fulfillment of the

Requirements for the Degree of

Doctor of Philosophy

in Mathematics

at

The University of Wisconsin-Milwaukee

May 2017

ABSTRACT

ON SOME ONE-COMPLEX DIMENSIONAL SLICES
OF THE BOUNDEDNESS LOCUS OF A MULTI-PARAMETER
RATIONAL FAMILY

by

Matthew Hoeppner

The University of Wisconsin-Milwaukee, 2017
Under the Supervision of Dr. Suzanne Boyd

Complex dynamics involves the study of the behavior of complex-valued functions when they are composed with themselves repeatedly. We observe the orbits of a function by passing starting values through the function iteratively. Of particular interest are the orbits of any critical points of the function, called critical orbits. The behavior of a family of functions can be determined by examining the change in the critical orbit(s) of the functions as the values of the associated parameters vary. These behaviors are often separated into two categories: parameter values where one or more critical orbits remain bounded, and parameter values where all critical orbits are unbounded. A famous example of this is the Mandelbrot set, which consists of all c-values at which the sole critical orbit of the polynomial $P_c(z) = z^2 + c$ is bounded.

In this paper we discuss some dynamics of the family of complex rational functions $R_{n,c,a}(z) = z^n + \frac{a}{z^n} + c$. If we fix the variables n and c while allowing a to vary, we see what look like small copies of the Mandelbrot set within the a-parameter plane. It turns out that for particular values of n, c, and a the function $R_{n,c,a}$ behaves locally like a quadratic polynomial. We prove that at these parameter values the 'baby' Mandelbrot sets which appear are in fact homeomorphic copies of the original Mandelbrot set.

We then examine other interesting parameter slices by fixing parameters or letting them vary in a predictable way. We once again observe the appearance of what look like Mandelbrot sets within these slices, and prove some properties regarding their locations.

TABLE OF CONTENTS

LIST OF FIGURES

ACKNOWLEDGEMENTS

First and foremost I would like to thank my advisor, Suzanne Boyd. She has been a wonderful source of help throughout the entirety of this process, and has always impressed me with the depth of her knowledge. She was incredibly patient and understanding with me at the times when I needed it most. She helped me to achieve something that I did not always think was possible, and for that I cannot offer enough thanks.

I would like to thank my committee members. Their advice and suggestions have been invaluable in getting this work into pristine shape.

I would like to thank my wife, Carlyn, for all her love and support, especially as she was often busier than I. I thank my parents, my sister, and my brother, whose belief always propelled me forward.

Chapter 1

Introduction

In Complex Dynamics we are interested in exploring the behavior of certain complex functions when they are composed with themselves repeatedly. We will begin with a brief summary of some important topics. A sound overview of the field is presented in texts such as [Bea91, GC93]. If we have a complex function $f(z)$, we find the n^{th} iterate of f by composing the function $f(z)$ repeatedly n times. That is, if we define $f^0(z) = z$, then $f^1(z) = f(z)$, $f^2(z) = f(f^1(z))$, and $f^n(z) = f(f^{n-1}(z))$.

In particular, we are interested in what happens to specific numbers when they are passed through the same function iteratively. Given a complex function $f(z)$ and an initial value z_0, we define the orbit of z_0 under $f(z)$ to be the infinite sequence $\{z_0, z_1 = f(z_0), z_2 = f(z_1), \ldots, z_n = f(z_{n-1}) = f^n(z_0), \ldots\}$. In studying the limiting behavior of an orbit as n grows large, several questions arise. Is the orbit bounded, or is it unbounded? If it remains bounded, does it tend towards a single point, a cycle of points, or does it behave in a way which cannot easily be described?

When examining the behavior of the orbits of a function, there are a few important subsets of $\overline{\mathbb{C}} = \mathbb{C} \cup \{\infty\}$ that we are interested in. The Fatou set of a function f consists of all values of z at which the family of iterates of f is normal on some neighborhood of z. In other words, z is in the Fatou set of f if every sequence of iterates of f has a subsequence

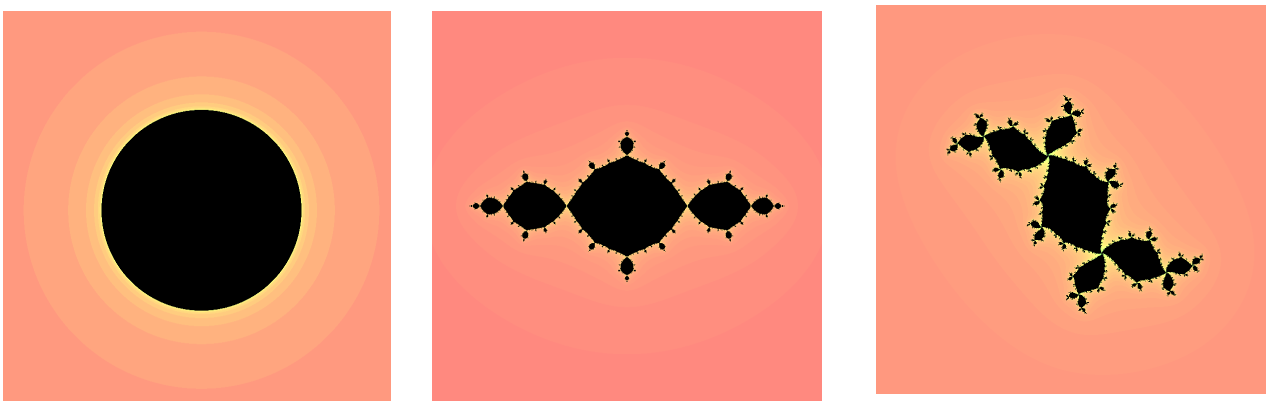

(a) Filled Julia set of P_0 (b) Filled Julia set of P_{-1} (c) Filled Julia set of $P_{-0.1+0.75i}$

Figure 1.1: A few filled Julia sets from $P_c = z^2 + c$

which converges uniformly on compact subsets of a neighborhood of z. This set can be thought of as the collection of z-values whose orbits are "well-behaved". The Julia set of a function f is simply the complement of the Fatou set, and contains the z-values whose orbits behave in ways that are not easily described. For polynomials, the filled Julia set is a set made up of the union of the Julia set of the polynomial along with any bounded components of the polynomial's Fatou set.

A common example used in Complex Dynamics is the polynomial $P_0(z) = z^2$. The behavior of most orbits in this example is very easy to see. Any starting value with a modulus that is less than one will have an orbit which tends towards zero. As we are working in $\overline{\mathbb{C}}$, any starting value with a modulus that is greater than one will have an orbit which tends towards infinity. All of these starting values are in the Fatou set of $P_0(z) = z^2$. If, however, we choose a point on the unit circle for a starting value, the behavior becomes harder to predict. Some orbits tend to a fixed point, some land on a cycle, and some never settle down. The unit circle is the Julia set of $P_0(z) = z^2$.

We can get an idea for what the filled Julia set of a polynomial looks like by drawing it with a computer program. The program DeTool[BB] gives a picture by iterating each point in the z-plane a large number of times and then coloring the point based on an educated guess as to whether the orbit of this point will grow beyond a predefined 'escape radius' or stay

bounded. Points whose orbits remain bounded are colored black, and points whose orbits 'escape' are shaded a lighter color, with different shades representing how many iterations it took for the orbit to extend outside this radius. The black regions represent the filled Julia set of the specified function, and the boundary between the black and colored regions of these figures represents the Julia set. Figure 1.1 shows some examples of various filled Julia sets; one from the polynomial $P_0(z) = z^2$ and two more from other polynomials in the family $P_c(z) = z^2 + c$, where $c \in \mathbb{C}$.

1.1 Dynamics in Families of Functions

In this paper we are more interested in exploring the dynamics of a family of functions rather than those of a single function. This, however, becomes more involved very quickly. Examining every orbit of every point for each function in the family would be an insurmountable task. Instead we study a family of functions by tracking the orbits of any critical points; that is, values of z for which $f'(z) = 0$. We do this by examining the change in these critical orbits as the parameters of the family vary.

A famous example is the family of complex polynomials $P_c(z)$. For P_c, regardless of the value of c, there is only one critical point; the one at $z = 0$. A simple way to classify this family is by identifying the region on which the unique critical orbit remains bounded. The set of c values for which the critical orbit of P_c is bounded is called the Mandelbrot set. This set can be visualized by creating a parameter plane for $P_c(z) = z^2 + c$. In this image every point represents a different c-value, and hence a different polynomial $z^2 + c$, and is colored depending on the boundedness of the critical orbit. For this reason, we also refer to this set as the boundedness locus for $z^2 + c$ (See Figure 1.2a).

Now consider a more general family of functions,

$$R_{n,c,a}(z) = z^n + \frac{a}{z^n} + c,$$

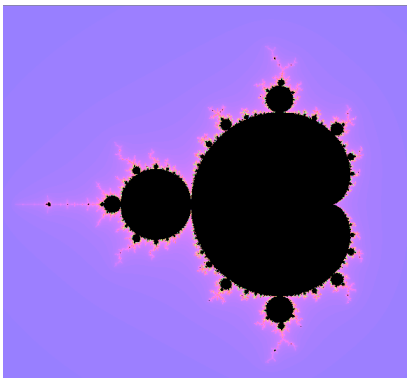

(a) The Mandelbrot Set

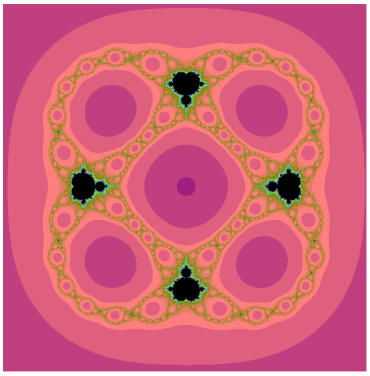

(b) The a-parameter plane when $n = 5$ and $c = 0$

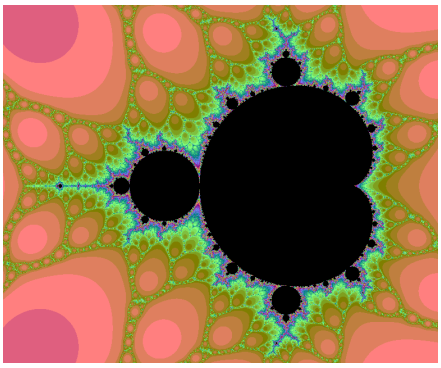

(c) A Mandelbrot Set within the a-plane of $R_{5,0,a}$

Figure 1.2: Parameter planes of P_c and $R_{5,0,a}$

where $a \in \mathbb{C} \setminus \{0\}$ and $c \in \mathbb{C}$. Fixing c to a constant, we see that this family has $2n$ critical points. While this seems like a lot of critical orbits to keep track of, in every case each of these critical points maps to one of just two critical values, $c + 2\sqrt{a}$ or $c - 2\sqrt{a}$, where we choose the branch cut of the square root function so that it is defined on $\mathbb{C} \setminus (-\infty, 0]$. This leaves us with just two critical orbits to consider.

The case of $c = 0$ has been studied extensively by Robert Devaney and his colleagues [Dev06, Dev13, Roe06, DBCF16, DBC$^+$14, Dev09, DR13, DBC$^+$13]. For any fixed n the critical values of $R_{n,0,a}$ are $\pm 2\sqrt{a}$, and as it happens the two critical orbits are either the same or symmetric. This makes it fairly easy to draw the a-parameter plane for these functions. For each a-value, we color a point on the a-parameter plane black if the critical orbits are bounded, or we shade the point with another color depending on the rate of escape. Just as for the family P_c, we call the black region in the a-parameter plane the boundedness locus (See Figure 1.2b for an example). If we zoom in on these images, we see what appear to be small 'copies' of the Mandelbrot set within these parameter planes (See Figure 1.2c). It has been proven that there are, in fact, multiple homeomorphic copies of the Mandelbrot set that appear throughout the boundedness locus [Dev06]. According to [DH85], this happens because there are neighborhoods of a-values for which the critical orbits of $R_{n,0,a}$ have the same dynamics as the critical orbit of P_c.

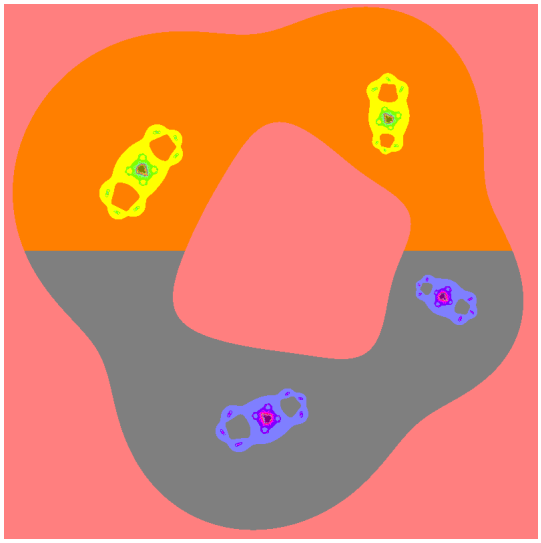

(a) The a-parameter plane of $R_{4,6i,a}$

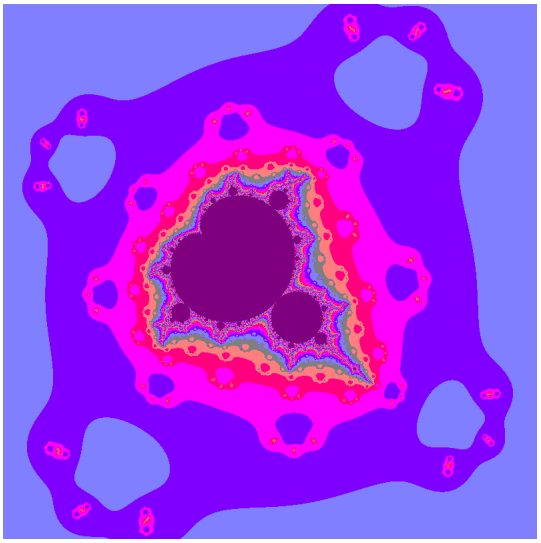

(b) A 'baby' Mandelbrot set in $R_{4,6i,a}$

Figure 1.3: A look at $R_{4,6i,a}$

1.2 Results

Throughout this paper we will be studying the family of functions $R_{n,c,a}(z) = z^n + \frac{a}{z^n} + c$, where $c \neq 0$. When c is non-zero, the boundedness locus becomes more complicated. The two critical orbits are now generated by the critical values $c \pm 2\sqrt{a}$. They are no longer symmetric and often behave very differently. However, we can put some constraints on the parameters to fix the behavior of one critical point. For example, it turns out that if $|c| > 1$, then one critical point always escapes. We use different colors to distinguish between the two critical orbits in the a-parameter plane (see Figure 1.3a, the color change is due to a branch cut of the square root function, since only one critical orbit is bounded in this plane). It appears as though homeomorphic copies of the Mandelbrot set exist here as well, each copy associated with one critical orbit (see Figure 1.3b). The number and position of these homeomorphic copies seem to change depending on the values of n and c. Al Mitchell has proven the existence of a copy of the Mandelbrot set in the a-plane for a small, fixed c, as well as the existence of many in the c-parameter plane for a range of fixed a-values [Mit16]. Some work has also been done on the Julia sets of this family for very particular parameter values [KD14, Dev14, BDGR08].

Given a certain set of constraints on the parameters of $R_{n,c,a}$ our ultimate goal in this paper is to prove the existence of homeomorphic copies of the Mandelbrot set within various one-complex dimensional slices of the (c, a)-parameter space of $R_{n,c,a}$ for fixed n. Background on some of the tools we will be using can be found in papers such as [Dev06, DH85, Shi87] With this goal in mind, there are four facets of each of these slices which can help us:

–First, we can identify a region in which the boundedness locus must lie. Any homeomorphic copies of the Mandelbrot set appearing in a slice of the (c, a) space of $R_{n,c,a}$ must necessarily occur within the boundedness locus, so confirming this region can help us to locate any Mandelbrot sets.

–Second, we can determine a curve, or 'spine', around which the boundedness locus is centered.

–Third, we can identify the collection of parameter values for which $c \pm 2\sqrt{a} = a^{1/2n}$ in a given slice. This helps us find the centers of our proposed baby Mandelbrot sets, which lets us create sets to contain each individual Mandelbrot set.

–Fourth and finally, we can show that each of these points corresponds to a baby Mandelbrot set.

Given a certain set of constraints we will attempt to find or verify as many of these properties as we can. Depending on the case some will be more difficult to find than others and not all of them are needed but we will show as many of them as we can.

We start off chapter 2 by presenting some preliminary findings from other papers. These are tools that are used regularly throughout this paper, including the method we use for proving the existence of small Mandelbrot sets within our slices.

In Chapter 3 we will begin our study in earnest with some results about the family of functions $R_{n,c,a}$ and the dynamical plane. This includes the development and description of two important sets, U'_a and U_a, to be used later in the paper.

Chapter 4 will bring us our first major results. When we look at images of Julia sets of $R_{n,c,a}$, we see what look like small copies of quadratic Julia sets. We first show that given

certain parameter restrictions, the Julia set of $R_{n,c,a}$ inside U'_a contains a homeomorphic copy of a quadratic Julia set. Two functions are considered topologically conjugate if they are conjugate via a homeomorphism. Specifically, we will show that U'_a contains a set on which $R_{n,c,a}$ is conjugate by means of a homeomorphism to some quadratic polynomial on its filled Julia set.

Theorem 4.3. *Let $n \geq 3$, $c \in \mathbb{R}$, $0 < c < \frac{|a|^{1/n}}{4}$, $|a| \leq 4$, and $arg(a) \neq \pi$. $R_{n,c,a}$ restricted to the set of points whose orbits remain in U'_a is topologically conjugate to some quadratic polynomial on its filled Julia set.*

Theorem 4.8. *Suppose $c \in \mathbb{R}$, $c < 0$, $|c| > 1 + \epsilon$, where $\epsilon > 0$ is small, and n sufficiently large so as to satisfy Proposition 4.6. Given these restrictions, $R_{n,c,a}$ restricted to the set of points whose orbits remain in U'_a is topologically conjugate to some quadratic polynomial on its filled Julia set.*

We finish Chapter 4 by establishing the existence of homeomorphic copies of the Mandelbrot set within the a-parameter plane of $R_{n,c,a}$ given a specific set of parameter restrictions. We will find that:

Theorem 4.15. *For $|c| \geq 6$ and n such that $4|c| + 8 \leq 2^{n+1}$, there exist n 'primary' homeomorphic copies of the Mandelbrot set in the boundedness locus in the a-plane of the family of functions $R_{n,c,a}(z) = z^n + \frac{a}{z^n} + c$.*

Next, we change our paradigm to allow both parameters a and c to vary in a one-dimensionally constrained way. In Chapter 5, we consider $c = ta$ for any non-zero complex slope t. Doing this also produces images which seem to contain homeomorphic copies of the Mandelbrot set (see Figure 1.4), but the boundedness locus is a bit more difficult to nail down. We don't confirm in this paper that these are copies of the Mandelbrot set, but we are able to establish multiple properties concerning the $c = ta$ slice for any non-zero t, including the designation of a curve, or 'spine', $\mathcal{S}_t$, which the boundedness locus must be near, as well as a neighborhood of this 'spine' wherein the boundedness locus must lie:

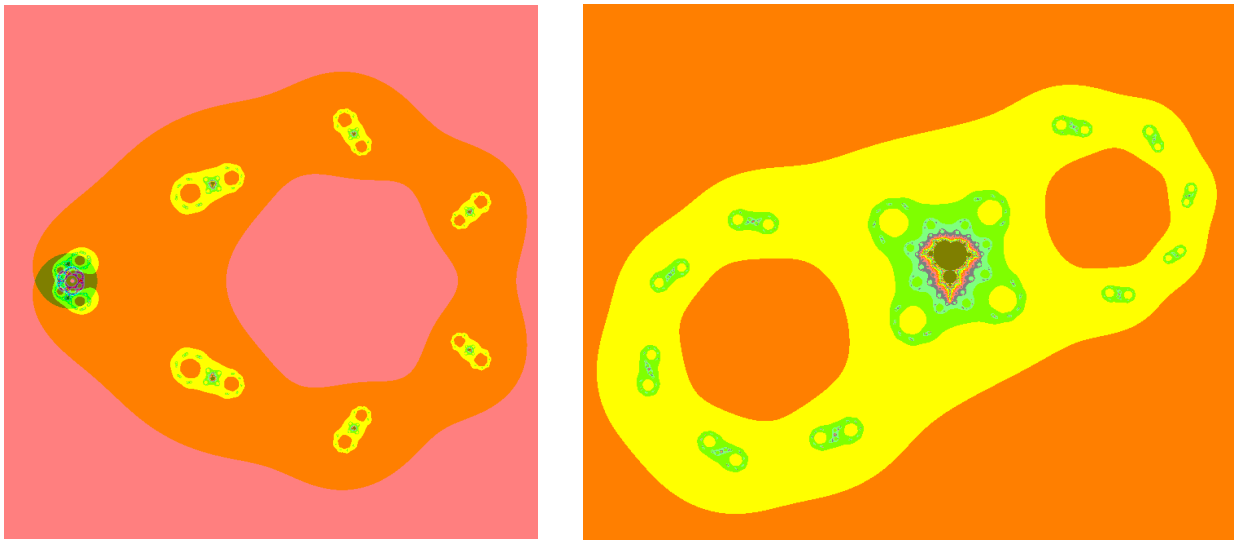

(a) Parameter plane slice for $n = 6$ (b) Zoomed in view

Figure 1.4: $R_{n,ta,a}(z) = z^n + \frac{a}{z^n} + ta$ with $n = 6$ and $t = 1$

Theorem 5.3. *Let $\epsilon > 0$. There exists an $N \geq 2$ such that for all $n \geq N$ we have $M_n(R_{n,ta,a}) \subset N_\epsilon(\mathcal{S}_t)$.*

Here $M_n(R_{n,ta,a})$ represents the boundedness locus of $R_{n,c,a}$ and $N_\epsilon(\mathcal{S}_t)$ designates an epsilon-neighborhood of the 'spine'.

Within chapter 6 we discuss a third way that this family can be viewed, which involves setting c so that the critical value $c + 2\sqrt{a}$ is always fixed. This also restricts us to a one-complex dimensional manifold in the (c, a) space, and gives us another set of images to describe the behavior of the family (see Figure 1.5). Looking at this subset, not only are there possible copies of the Mandelbrot set strewn throughout these parameter planes, but what appear to be homeomorphic copies of Julia sets of P_c. Recall the Julia set of $P_0(z) = z^2$ is the unit disk. This is the Julia set with one fixed critical point. Note the appearance of unit disks as well as small copies of the Mandelbrot set in Figure 1.5a. This seems not to be a coincidence as one of our critical values here is always fixed. Since the critical value $c + 2\sqrt{a}$ is fixed the behavior is determined entirely by the critical orbit of $c - 2\sqrt{a}$. We will find these Mandelbrot 'copies' by looking for where $c - 2\sqrt{a}$ is also fixed. It turns out that these locations can be classified in two ways:

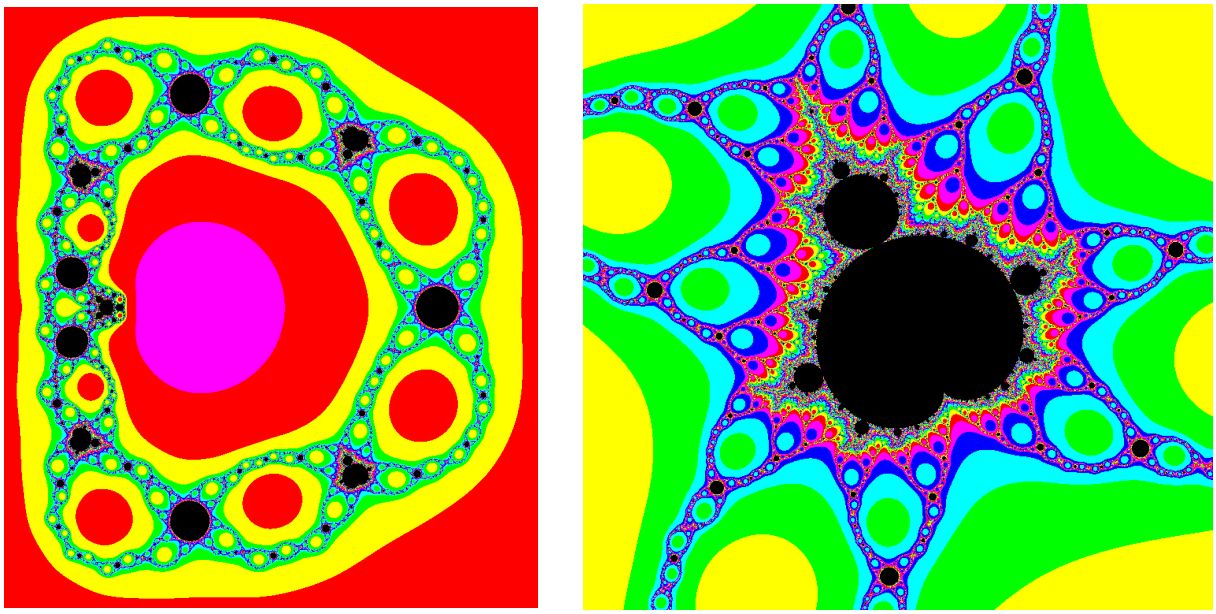

(a) Parameter plane for $n = 6$

(b) Zoomed in on 'Mandelbrot' set

Figure 1.5: The parameter plane for $R_{6,a}$

Theorem 6.3. *Let*

$$a = \left(\frac{1 - e^{i\frac{k\pi}{n}}}{4} \right)^{\frac{2n}{n-1}} \quad \textit{for} \quad k = 1, 2, 3, ..., 2n-1,$$

and define $c = a^{1/2n} - 2\sqrt{a}$. *Then for each* $k = 1, 2, 3, ..., 2n-1$, *if* k *is odd then the critical value* $c - 2\sqrt{a}$ *is fixed at a non-canonical root of* $a^{1/2n}$. *If* k *is even, then* $c - 2\sqrt{a}$ *maps to* $c + 2\sqrt{a}$.

Note: by the canonical $2n^{\text{th}}$ root of a we mean $|a|^{\frac{1}{2n}} e^{i\frac{arg(a)}{2n}}$.

Lastly, chapter 7 briefly discusses a few future avenues of study. We look at some interesting but as-yet unexplained behaviors, including the presence of what look like homeomorphic copies of quadratic Julia sets appearing in the one-dimensional slices of $R_{n,c,a}$.

Chapter 2

Preliminaries

The proofs of the ideas presented in this paper rely on observations made in other papers, as well as on the use of tools developed by others. A description of the tools and observations that will be used is presented in this chapter.

2.1 Polynomial-Like Maps

In the paper [Dev06], Robert Devaney uses tools developed by Douady and Hubbard in [DH85] to show that small copies of the Mandelbrot set, or 'baby' Mandelbrot sets, exist within the parameter planes of $R_{n,0,a}$. The use of these tools revolves around showing that a particular family of functions behaves locally like a degree two polynomial. In order to show that a function or family of functions behaves like a polynomial we first need the definition of a polynomial-like mapping.

Definition 2.1. *[DH85] A polynomial-like map of degree d is a proper, analytic map of degree d, $f : U' \to U$, where U' and U meet the following conditions: both U' and U are open subsets of $\mathbb{C}$ which are homeomorphic to disks, $U' \subset U$, and U' is relatively compact in U.*

Each polynomial-like map of degree d has exactly $d-1$ critical points. For our purposes we will only be concerned with polynomial-like maps of degree two. A polynomial-like map

of degree two is a two-to-one map from U' to U, and has a unique critical point in U'. We also have a different definition for the filled Julia set of a polynomial-like map. The filled Julia set of a polynomial-like map is defined as the collection of points in U' whose orbits never leave U'. While it is not immediately obvious that this definition of a polynomial-like map produces functions which behave like polynomials, the following proposition shows that it is an apt name.

Proposition 2.2. *[DH85] A polynomial-like map of degree two is topologically conjugate on its filled Julia set to some quadratic polynomial on the polynomial's filled Julia set.*

This show us that such polynomial-like maps of degree two do behave locally like degree two polynomials. Taking this and looking at a family of such maps gives a very interesting result, as stated by Robert Devaney based on work done by Douady and Hubbard:

Theorem 2.3. *[Dev06][DH85] Suppose we have a family of polynomial-like maps $f_\lambda : U'_\lambda \to U_\lambda$ which satisfy the following:*

(1) The parameter λ is contained in an open set in $\mathbb{C}$ which contains a closed disk W;

(2) The boundaries of U'_λ and U_λ both vary analytically as λ varies;

(3) The map $(\lambda, z) \to f_\lambda(z)$ depends analytically on λ and z;

(4) Each f_λ is polynomial-like of degree two and has a unique critical point, c_λ.

Suppose that for each λ in the boundary of W we have that $f_\lambda(c_\lambda) \in U_\lambda - U'_\lambda$, and that $f_\lambda(c_\lambda)$ winds once around U'_λ (and therefore once around c_λ) as λ winds once around the boundary of W. Then the set of all λ for which the orbit of c_λ does not escape from U'_λ is homeomorphic to the Mandelbrot set.

This theorem gives us a method for proving that a given parameter plane contains homeomorphic copies of the Mandelbrot set. If we can find regions U'_λ and U_λ on which our family of functions is polynomial-like and show that the rest of these properties hold, then we can show that a copy of the Mandelbrot set exists. Robert Devaney used this method to show that the a-parameter plane of $R_{n,0,a}$ contains $n-1$ small copies of the Mandelbrot set for

all $n \geq 3$. In fact, there appear to be many more than just $n-1$ copies, but these $n-1$ are the largest and most obvious and so he refers to them as the $n-1$ 'principal' copies of the Mandelbrot set.

2.2 Preliminaries Regarding $R_{n,c,a}$

In their paper [BS11], Boyd and Schulz provide a number of results on the properties of the family of functions $R_{n,c,a}(z) = z^n + \frac{a}{z^n} + c$, as well as on the Julia sets of said family. There are two results from this paper which are of particular interest here. The first provides information about the location of the filled Julia sets of $R_{n,c,a}$ for sufficiently large n.

Corollary 2.4. *[BS11] For any $c \in \mathbb{C}$ and any $a \in \mathbb{C}^*$, given any $\epsilon > 0$, there is an $N \geq 2$ such that for all $n \geq N$, we have that $K(R_{n,c,a})$, the filled Julia set of $R_{n,c,a}$, is contained within an annulus near the unit circle: $K(R_{n,c,a}) \subset \mathbb{A}(1-\epsilon, 1+\epsilon)$.*

For any choice of c, a, and ϵ, if n is sufficiently large then the filled Julia set of $R_{n,c,a}$ must be contained within an ϵ-annulus around S^1. This helps us with determining a boundedness locus for $R_{n,c,a}$ for any choice of parameters, so long as n is large enough. In later chapters when we explore a few modifications of the family $R_{n,c,a}$ this property of the Julia set will still hold and will therefore allow us to use the same method for finding the boundedness locus then as well.

The second result allows us to sometimes locate the centers of the baby Mandelbrot sets in the a-plane of $R_{n,c,a}$. For $R_{n,0,a}$, Devaney used the fact that one of the baby Mandelbrot sets always appears centered on the real axis as well as a rotational argument to locate the $n-1$ principal copies. When we perturb $R_{n,0,a}$ with a nonzero c, this no longer works. Another method is needed in order to locate the baby Mandelbrot sets.

Lemma 2.5. *[BS11] For any $|c| \geq 1$ and $n \geq 2$, there exist n distinct solutions in the family of functions $R_{n,c,a}$ to the equations $c \pm 2\sqrt{a} = a^{1/2n}$.*

In other words, there are n fixed critical points in the a-plane given $|c| \geq 1$ and $n \geq 2$. When we use Douady and Hubbard's method 2.3 for identifying homeomorphic copies of the Mandelbrot set these copies come from a collection of a-values for which the orbit of the critical point $a^{1/2n}$ does not escape from the set U'_a. Therefore it is natural to expect any parameter value which causes a fixed critical point to stand as a 'center' around which a baby Mandelbrot set should exist in the a-parameter plane. This is what we will use to create a U' which encapsulates what we will call a 'baby' Julia set.

Chapter 3

Dynamical Plane Results

For any particular family of functions the list of goals, as mentioned earlier, is as follows: We would like to identify a region of the parameter space on which the boundedness locus must lie. We would like to determine a curve, or 'spine', around which the boundedness locus is centered. We would like to identify the collection of a-values for which $c \pm 2\sqrt{a} = a^{1/2n}$, which helps us find the centers of our proposed baby Mandelbrot sets. Finally, we would like to show that each of these points corresponds to a baby Mandelbrot set. In each case we would like to find as many of these things as we can, with the ultimate goal being to prove the existence of baby Mandelbrot sets.

We will first set forth a few properties concerning $R_{n,c,a}$ which will remain useful throughout the rest of this paper. Specifically, we will look at the dynamical plane, and lay groundwork for describing U' and U.

3.1 Involution of $R_{n,c,a}$ and the Sets U' and U

As we saw in the Preliminaries, in order to prove that we have a baby Mandelbrot set we will need to create two sets, U' and U, and prove that they satisfy several conditions. The set U' must be crafted carefully, as it needs to encapsulate a baby Julia set, but must also map two-to-one onto U.

Definition 3.1. *Given any family of functions $R_{n,c,a}$, let $arg(a) = \psi$ and define*

$$U'_a = \left\{ z \;\middle|\; \frac{|a|^{\frac{1}{n}}}{2} < |z| < 2,\ \frac{\psi - \pi}{2n} < Arg(z) < \frac{\psi + \pi}{2n} \right\},$$

and

$$U_a = R_{n,c,a}(U'_a).$$

These definitions for U'_a and U_a are the same ones used by Robert Devaney in [Dev06]. Note that U'_a does not depend on c, but of course its image, U_a, does. When we use a nonzero value for the parameter c, the description of the set U_a becomes a lot more complicated. A proper description of the set is important, as later on we will need to show that U'_a is contained within U_a under certain parameter constraints. We also need to show that this U'_a does in fact map two-to-one onto U_a. In order to do either of these things we first need to establish an important property of the family of functions $R_{n,c,a}$.

Proposition 3.2. *The family of functions $R_{n,c,a}$ is symmetric under the involution $h_a(z) = \frac{a^{1/n}}{z}$.*

Proof.

$$R_{n,c,a}\left(\frac{a^{1/n}}{z}\right) = \left(\frac{a^{1/n}}{z}\right)^n + \frac{a}{\left(\frac{a^{1/n}}{z}\right)^n} + c = \frac{a}{z^n} + z^n + c = R_{n,c,a}(z).$$

□

This property is what allows us to create a U'_a which maps two-to-one onto its image under $R_{n,c,a}$. If we look at the two circles $|z| = 2$ and $|z| = \frac{a^{\frac{1}{n}}}{2}$, we see that due to this involution both of these circles map to the same curve under $R_{n,c,a}$. The 'inner' and 'outer' boundaries of U'_a lie on each of these circles. These two arcs of the boundary of U'_a are involutions of each other, so they both map to the same curve in U_a. A full description of U_a, and how U'_a maps onto it, follows.

Proposition 3.3. *The ellipse parameterized by*

$$x = \left(2^n + \frac{|a|}{2}\right)\cos(\theta)$$
$$y = \left(2^n - \frac{|a|}{2}\right)\sin(\theta)$$

is an ellipse centered at 0 *where the semi-major axis lies along the x-axis and has length* $\left(2^n + \frac{|a|}{2}\right)$*, and the semi-minor axis lies along the y-axis and has length* $\left(2^n - \frac{|a|}{2}\right)$*. Define the ellipse* $\mathcal{E}$ *to be this ellipse, shifted so that it is centered at c, and rotated counter-clockwise by* $\frac{\psi}{2}$*. The set* $U_a = R_{n,c,a}(U_a')$ *is one half of the ellipse* $\mathcal{E}$*, including the minor axis. Additionally,* $R_{n,c,a}$ *maps* U_a' *two-to-one onto* U_a*.*

Proof. First we examine the images of the outer and inner boundary arcs of U_a'. Note that, due to the involution map, $h_a(z)$, both the outer arc which lies on $|z| = 2$ and the inner arc which lies on $|z| = \frac{a^{1/n}}{2}$ are mapped to the same curve by $R_{n,c,a}$. Ignoring for a moment the restriction on the argument we will look at $\left\{R_{n,c,a}(2e^{i\theta}) \mid 0 \le \theta \le 2\pi\right\}$. Since we are considering all values of θ, we can add a rotation to the angle of θ and still end up with the same image. Thus, we instead consider the following:

$$\begin{aligned}
R_{n,c,a}\left(2e^{i(\theta+\frac{\psi}{2n})}\right) &= \left(2e^{i(\theta+\frac{\psi}{2n})}\right)^n + \frac{a}{\left(2e^{i(\theta+\frac{\psi}{2n})}\right)^n} + c \\
&= 2^n e^{i(n\theta+\frac{\psi}{2})} + \frac{|a|e^{i\psi}}{2^n e^{i(n\theta+\frac{\psi}{2})}} + c \\
&= 2^n e^{in\theta}e^{i\frac{\psi}{2}} + \frac{|a|e^{i\frac{\psi}{2}}}{2^n e^{in\theta}} + c \\
&= e^{i\frac{\psi}{2}}\left(2^n e^{in\theta} + \frac{|a|}{2}e^{-in\theta}\right) + c \\
&= e^{i\frac{\psi}{2}}\left(2^n\left(\cos(n\theta) + i\sin(n\theta)\right) + \frac{|a|}{2}\left(\cos(n\theta) - i\sin(n\theta)\right)\right) + c \\
&= e^{i\frac{\psi}{2}}\left(\left(2^n + \frac{|a|}{2}\right)\cos(n\theta) + \left(2^n - \frac{|a|}{2}\right)i\sin(n\theta)\right) + c.
\end{aligned}$$

Now we focus on just $\left(2^n + \frac{|a|}{2}\right)\cos(n\theta) + \left(2^n - \frac{|a|}{2}\right) i\sin(n\theta)$ for a moment. We can parameterize this as:

$$x = \left(2^n + \frac{|a|}{2}\right)\cos(n\theta)$$
$$y = \left(2^n - \frac{|a|}{2}\right)\sin(n\theta).$$

This is the parameterization for an ellipse centered at 0 where the semi-major axis lies along the x-axis and has length $\left(2^n + \frac{|a|}{2}\right)$, the semi-minor axis lies along the y-axis and has length $\left(2^n - \frac{|a|}{2}\right)$, and which is traversed n times as θ goes from 0 to 2π. Going back to

$$e^{i\frac{\psi}{2}}\left(\left(2^n + \frac{|a|}{2}\right)\cos(n\theta) + \left(2^n - \frac{|a|}{2}\right) i\sin(n\theta)\right) + c,$$

we see that this is the same ellipse rotated by an angle of $\frac{\psi}{2}$ and shifted by c. Thus $\left\{R_{n,c,a}(2e^{i\theta}) | 0 \leq \theta \leq 2\pi\right\}$ gives us an ellipse with a semi-major axis of length $\left(2^n + \frac{|a|}{2}\right)$ and a semi-minor axis of length $\left(2^n - \frac{|a|}{2}\right)$ which has been rotated by an angle of $\frac{\psi}{2}$, which is traversed n times, and which is centered at c. This is exactly our ellipse $\mathcal{E}$. Notice that the foci of this ellipse are at $c \pm 2\sqrt{a}$, which are the two critical values of $R_{n,c,a}$! Now, the image under $R_{n,c,a}$ of both circles of radius 2 and $\frac{a^{1/n}}{2}$ covers $\mathcal{E}$ a total of n times, but the boundary of U'_a only occupies $\frac{1}{2n}$th of each circle. Thus the image of the inner and outer arcs of U'_a is exactly half of this ellipse $\mathcal{E}$.

Next we examine the images under $R_{n,c,a}$ of the two rays in the boundary of U'_a. The images of each of these rays are given by

$$\left\{R_{n,c,a}\left(re^{i\left(\frac{\psi \pm \pi}{2n}\right)}\right) \;\middle|\; \frac{a^{1/n}}{2} \leq r \leq 2\right\}.$$

Evaluating each of these gives us

$$\begin{aligned} R_{n,c,a}\left(re^{i\left(\frac{\psi+\pi}{2n}\right)}\right) &= r^n e^{i\left(\frac{\psi+\pi}{2}\right)} + \frac{a}{r^n e^{i\left(\frac{\psi+\pi}{2}\right)}} + c \\ &= r^n e^{i\left(\frac{\psi}{2}+\frac{\pi}{2}\right)} + \frac{|a|e^{i\psi}}{r^n e^{i\left(\frac{\psi}{2}+\frac{\pi}{2}\right)}} + c \\ &= e^{i\frac{\psi}{2}}\left(r^n e^{i\left(\frac{\pi}{2}\right)} + \frac{|a|}{r^n e^{i\left(\frac{\pi}{2}\right)}}\right) + c \\ &= e^{i\frac{\psi}{2}}\left(r^n - \frac{|a|}{r^n}\right) i + c, \end{aligned}$$

and

$$\begin{aligned} R_{n,c,a}\left(re^{i\left(\frac{\psi-\pi}{2n}\right)}\right) &= r^n e^{i\left(\frac{\psi-\pi}{2}\right)} + \frac{a}{r^n e^{i\left(\frac{\psi-\pi}{2}\right)}} + c \\ &= r^n e^{i\left(\frac{\psi}{2}-\frac{\pi}{2}\right)} + \frac{|a|e^{i\psi}}{r^n e^{i\left(\frac{\psi}{2}-\frac{\pi}{2}\right)}} + c \\ &= e^{i\frac{\psi}{2}}\left(r^n e^{i\left(-\frac{\pi}{2}\right)} + \frac{|a|}{r^n e^{i\left(-\frac{\pi}{2}\right)}}\right) + c \\ &= -e^{i\frac{\psi}{2}}\left(r^n - \frac{|a|}{r^n}\right) i + c. \end{aligned}$$

Each of these is a line segment along the imaginary axis which is then rotated by $\frac{\psi}{2}$ and shifted by c. The images of the two boundary rays correspond both to the same line segment, traversed in opposite directions as $r : \frac{a^{1/n}}{2} \mapsto 2$. Before rotation by $\frac{\psi}{2}$ and translation by c, the line segment $\left(r^n - \frac{|a|}{r^n}\right) i$ as $r : \frac{a^{1/n}}{2} \mapsto 2$ is the line segment between $\left(2^n - \frac{|a|}{2^n}\right) i$ and $-\left(2^n - \frac{|a|}{2^n}\right) i$. After rotation and translation, this is exactly the minor axis of the ellipse $\mathcal{E}$! Thus, $R_{n,c,a}(U'_a) = U_a$ is half an ellipse, divided along the minor axis, which is centered at c and rotated by $\frac{\psi}{2}$. Moreover, $R_{n,c,a}$ maps U'_a two-to-one onto U_a. □

Figure 3.1 gives an idea of what both $\mathcal{E}$ and U_a look like. With these results established

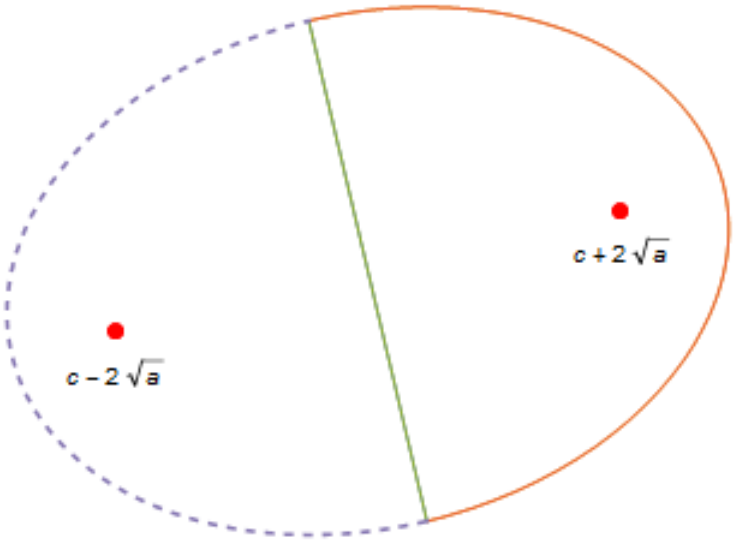

Figure 3.1: Visualization of $\mathcal{E}$ and U_a.

we can now turn to studying the dynamics of $R_{n,c,a}$. The first step will be to study $R_{n,c,a}$ while being as loose as possible as far as restrictions on the parameters.

3.2 The Escape Radius

First we will establish some properties of the filled Julia sets of $R_{n,c,a}$ which will remain true regardless of the future restrictions that we put on the parameters. These will be generalizations of results in [BS11]. To that end we will let $a \in \mathbb{C} \setminus \{0\}$, $c \in \mathbb{C}$, and $n \geq 3$. Throughout this paper we will ignore the cases $n = 1$ and $n = 2$, as the dynamics are less interesting and not in line with the results for any larger values of n, respectively. Robert Devaney gives reasons as to why the case $n = 2$ is 'crazy' in his paper [Dev12].

The point at infinity is a super-attracting fixed point, meaning that the derivative when

evaluated at infinity is zero. For infinity, this is determined by conjugating with the function $z \to \frac{1}{z}$ and calculating the derivative at zero. This fact does not hold true when $n = 1$ and is one reason that case is left out. Infinity being super-attracting implies that there is some 'escape' radius beyond which the orbits of z must tend towards infinity. Therefore each Julia set is bounded, and must avoid some neighborhood of infinity. In this first result we calculate a neighborhood of the origin in which a particular Julia set must lie depending on the parameters that are chosen.

Lemma 3.4. *For any $c \in \mathbb{C}$, any $a \in \mathbb{C}\backslash\{0\}$, and any integer $n \geq 3$, set $s = max\{4, |c|, |a|\}$. Then for any $|z| \geq s$, the orbit of z under $R_{n,c,a}$ escapes to infinity.*

Proof. Fix $c \in \mathbb{C}$, $a \in \mathbb{C}$, and $n \geq 3$. Suppose that $|z| \geq s$. Note then that $s^{n-2} \geq 4$ for any choice of $n \geq 3$. I claim that $|R^m_{n,c,a}(z)| > s^m$ for all $m \geq 1$. First,

$$\begin{aligned}
|R_{n,c,a}(z)| &= \left|z^n + c + \frac{a}{z^n}\right| \\
&\geq |z|^n - |c| - \frac{|a|}{|z|^n} \\
&> 3s - s - \frac{|a|}{3s} \\
&> 3s - s - \frac{|a|}{s} \\
&= 2s - \frac{|a|}{s} \\
&= s + \left(s - \frac{|a|}{s}\right) \\
&> s.
\end{aligned}$$

Now, suppose for some $m \geq 1$, $|R^m_{n,c,a}(z)| > s^m$. Then,

$$\begin{aligned}
|R^{m+1}_{n,c,a}(z)| &= \left|(R^m_{n,c,a}(z))^n + c + \frac{a}{(R^m_{n,c,a}(z))^n}\right| \\
&\geq |R^m_{n,c,a}(z)|^n - |c| - \frac{|a|}{|R^m_{n,c,a}(z)|^n} \\
&> s^{mn} - s - \frac{|a|}{s^{mn}} \\
&\geq s^{mn-m+1} - s - \frac{|a|}{s^{mn}} \\
&= s^{m(n-1)+1} - s - \frac{|a|}{s^{mn}} \\
&= s^{m+1}\left(s^{m(n-2)} - s^{-m} - \frac{|a|}{s^{mn+m+1}}\right) \\
&> s^{m+1}(4^m - 1 - 1) \\
&> s^{m+1}.
\end{aligned}$$

Thus by induction, $|R^m_{n,c,a}(z)| > s^m$ for all $m \geq 1$. Since $s \geq 4$, the orbit of z under $R_{n,c,a}$ escapes to infinity. Thus we have that for any choice of z such that $|z| > s$, the orbit of z under $R_{n,c,a}$ will escape to infinity. □

Next we notice that, since 0 is a preimage of infinity, there must be a neighborhood of 0 which maps beyond the escape radius established in Lemma 3.4. Thus there must be a neighborhood of 0 which the Julia set avoids as well. We can find this 'inner' radius by using the involution that we introduced in the previous section.

Lemma 3.5. *For any $c \in \mathbb{C}$, any $a \in \mathbb{C} \setminus \{0\}$, and any integer $n \geq 3$, set $t = \frac{|a|^{1/n}}{s}$, where s is defined as in Lemma 3.4. Then $t < s$, and for any $|z| \leq t$ the orbit of z under $R_{n,c,a}$ escapes to infinity.*

Proof. First, suppose that $|a| < 1$. Then $|a|^{1/n} < 1$, and since $s \geq 4$ we have $t < 1$, and thus $t < s$. Now suppose $|a| = 1$. Then $t = \frac{|a|^{1/n}}{s} = \frac{1}{s} < 1$, so $t < s$. Finally, suppose $|a| > 1$. Then $|a|^{1/n} < |a|$, so $t = \frac{|a|^{1/n}}{s} < \frac{|a|}{s}$. Since $s \geq |a|$, we have $t < 1$ again, so $t < s$. Thus not only is $t < s$, but we have $t < 1$ for any choice of n, c, a.

Next, let z be such that $|z| \leq t$. Then

$$|H_a(z)| = \frac{|a|^{1/n}}{|z|} \geq \frac{|a|^{1/n}}{t} = \frac{|a|^{1/n}}{\frac{|a|^{1/n}}{s}} = s.$$

Thus, by Lemma 3.4, the orbit of $H_a(z)$ under $R_{n,c,a}$ escapes to infinity. Now, the involution has the property that $R_{n,c,a}(z) = R_{n,c,a}(H_a(z))$, so since the orbit of $H_a(z)$ escapes to infinity, so does the orbit of z. □

Combining these two results gives us an annulus in which the filled Julia set must exist for some particular choice of parameters.

Proposition 3.6. *Let $c \in \mathbb{C}$, $a \in \mathbb{C} \setminus \{0\}$, and $n \geq 3$. Let s and t be defined as in 3.4 and 3.5. For any choice of parameters the filled Julia set of $R_{n,c,a}$ must be contained within the annulus $\mathbb{A}(t, s) = \{z \in \mathbb{C} \mid t < |z| < s\}$.*

Proof. This result follows directly from Lemmas 3.4 and 3.5. □

Chapter 4

Baby Julia Sets and Baby Mandelbrot Sets for $R_{n,c,a} = z^n + \frac{a}{z^n} + c$ with c Fixed

In this chapter we present our first example of following the procedure that we have set forth. We will investigate the boundedness locus of $R_{n,c,a}$ and the presence of baby Mandelbrot sets in the case that the parameter space is the a-plane; that is, the one-complex dimensional plane with the parameters c and n fixed while the parameter a varies.

4.1 The Boundedness Locus and U_a' in U_a

We have established definitions for U_a' and U_a and given a description of what U_a looks like. We know that U_a' maps two-to-one onto U_a, but we have not established that $U_a' \subset U_a$ for any choice of a. This proved too difficult to show in so general a fashion. Therefore, whenever we introduce a new set of restrictions on the parameters of $R_{n,c,a}$, one of the first things we do is to prove that $U_a' \subset U_a$ using our new restrictions. In this section we will show that $U_a' \subset U_a$ for a couple of parameter restrictions, hence establishing the existence of some baby Julia sets within the Julia sets of $R_{n,c,a}$. We will also find a boundedness locus that works for a very wide range of parameter values.

The results in this section must be split into two groups based on the value of the

parameter c. The dynamics of $R_{n,c,a}$ depend on c not only in a direct sense, but also in a more general fashion. The type and quantity of principal Mandelbrot sets that appear in the a-plane of $R_{n,c,a}$ changes depending on whether c is very small or relatively large. This change in behavior happens around $|c| = 1$. As we saw in chapter 2, when $c \geq 1$ we can show that there are n solutions to the equations $c \pm 2\sqrt{a} = a^{1/2n}$, which correspond to n principal baby Mandelbrot sets. However, when $|c| < 1$, some of these principal baby Mandelbrot sets start to merge and deform, resulting in shapes which have some similarities to the Mandelbrot set, but which are noticeably different.

For the most part we will be focusing on the dynamics when $|c| > 1$. Determining the dynamics for $|c| < 1$ requires a change in method and so is only explored briefly in this thesis. Nevertheless, we do have some results for some small values of c.

4.1.1 Results for Small c

One of the things we look at for small c-values is to show that U_a' is contained in U_a given certain restrictions. Showing that $U_a' \subset U_a$ will often happen in two parts. First we will show that U_a' is contained in the ellipse $\mathcal{E}$, and then show that it does not touch the minor axis of $\mathcal{E}$.

Proposition 4.1. *Let $|c| < t$ as defined in Lemma 3.5 and let $|a| \leq 4$. Then for any choice of $n \geq 3$, U_a' is contained in $\mathcal{E}$.*

Proof. Suppose $|c| < t = \dfrac{|a|^{1/n}}{s}$ and $|a| \leq 4$. Then $s = max\{4, |c|, |a|\} = 4$ so $|c| < \dfrac{|a|^{1/n}}{4}$. The shortest distance from the center, c, of $\mathcal{E}$ to the boundary is given by the length of the semi-minor axis, which is $2^n - \dfrac{|a|}{2^n}$. Since $n \geq 3$, $2^{n+1} - \dfrac{1}{2^{n-1}} > 2^n - \dfrac{1}{2^{n-2}}$ for any choice of n.

Thus,

$$2^n - \frac{|a|}{2^n} \geq 2^n - \frac{4}{2^n} = 2^n - \frac{1}{2^{n-2}} \geq 8 - \frac{1}{2} = \frac{15}{2}.$$

Next, suppose $|z| = 2$. Then $|c - z| \leq |c| + |z| < \dfrac{|a|^{1/n}}{s} + 2 < 1 + 2 = 3$. We now have that

the distance from from c to any point on the circle $\{z \mid |z| = 2\}$ is less than 3, and the length of the semi-minor axis of $\mathcal{E}$ is greater than $\frac{15}{2}$. Thus $\mathcal{E}$ contains $\{z \mid |z| \leq 2\}$, and therefore contains U'_a. □

Unfortunately, letting c be complex makes it a little too difficult to show that U'_a is contained in U_a. If instead we have c be real then we can finish with this result.

Proposition 4.2. *Let $c \in \mathbb{R}$, $0 < c < t$, $|a| \leq 4$, $n \geq 3$, and $-\pi < \psi \leq \pi$. Then $U'_a \subset U_a$.*

Proof. These restrictions on c, a, and n satisfy the requirements of Proposition 4.1, so U'_a must be contained in $\mathcal{E}$. We have assumed that $|a| \leq 4$, so certainly we have $|a|^{1/2n} < 4$. From this we can say that $\frac{|a|^{1/n}}{4} < |a|^{1/2n}$ and therefore $c < |a|^{1/2n}$ for all available choices of a. The set U'_a has been built so that it always contains the critical point $a^{1/2n}$. A simple calculation shows that $a^{1/2n}$ maps to the critical value $c + 2\sqrt{a}$ (the 'positive' focus of $\mathcal{E}$). Since $c \in \mathbb{R}$, if we choose an a so that $a \in \mathbb{R}$ as well we get an $\mathcal{E}$ which is centered on the real axis with its major axis lying on $\mathbb{R}$. Since $c < |a|^{1/2n}$ this means that whenever a is real we can say that $U'_a \cap U_a \neq \emptyset$. If we can show that the minor axis of $\mathcal{E}$ does not intersect U'_a then by continuity we can say that $U'_a \subset U_a$. To show this, fix $|a|$ and set $\psi = 0$. Here U'_a rests on the real axis, with the two ray boundaries at arguments $\pm\frac{\pi}{2n}$. The ellipse $\mathcal{E}$ has its major axis on the real axis, and its minor axis, which makes up part of the boundary of U_a, running vertically through c. See Figure 4.1 for an example of $\mathcal{E}$, U'_a, and U_a.

The minor axis of $\mathcal{E}$ intersects the circle $\left\{ z \;\middle|\; |z| = \dfrac{|a|^{1/n}}{2} \right\}$ in two places. Let $\pm\theta$ be the arguments of the intersection points. Since we have $c < \dfrac{|a|^{1/n}}{4}$,

$$\cos(\pm\theta) < \frac{\frac{|a|^{1/n}}{4}}{\frac{|a|^{1/n}}{2}} = \frac{1}{2}.$$

Thus, $\theta > \frac{\pi}{3}$. Since $n \geq 3$, the ray boundaries of U'_a have arguments between $\pm\frac{\pi}{6}$. Since the minor axis does not intersect U'_a on $\left\{ z \;\middle|\; |z| = \dfrac{|a|^{1/n}}{2} \right\}$, it does not intersect it anywhere and thus $U'_a \subset U_a$ when $\psi = 0$.

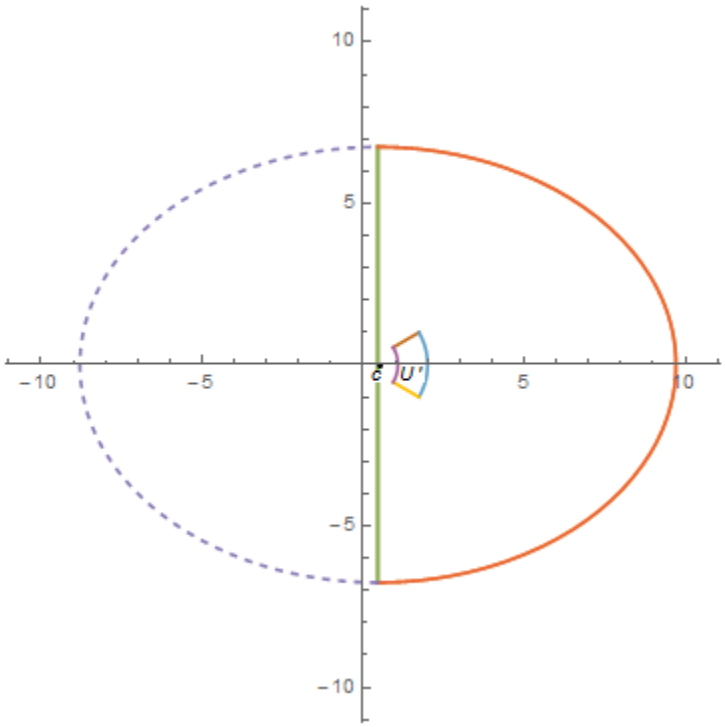

Figure 4.1: $\mathcal{E}$ with major axis on $\mathbb{R}$

Next we will let ψ go from 0 to π. In doing this $\mathcal{E}$ is rotated by $\frac{\psi}{2}$, so as ψ increases, the argument of U_a with respect to c increases by $\frac{\psi}{2}$. On the other hand, as ψ increases the argument of U'_a increases by at most $\frac{\pi}{6}$ as n must be at least 3. Thus while the upper ray boundary of U'_a will not catch up with the positive semi-minor axis, it is possible that the negative semi-minor axis will catch up with the lower ray boundary of U'_a. This can happen at just one single value of ψ. Let us now examine U'_a and U_a when $\psi = \pi$. When $\psi = \pi$, U_a has been rotated by $\frac{\pi}{2}$, so the minor axis of $\mathcal{E}$ lies on the real axis. The upper ray boundary of U'_a has argument $\leq \frac{\pi}{3}$ and the lower ray boundary of U'_a has argument 0. See Figure 4.2.

Since the argument of U'_a and U_a both increase linearly, this is the first and only time that the boundary of U_a touches the boundary of U'_a. Thus for $0 \leq \psi < \pi$ we have $U'_a \subset U_a$. Furthermore, when $\psi = \pi$ the boundaries of U'_a and U_a touch, but both U'_a and U_a are open so we still have $U' \subset U$.

Finally we will let ψ go from 0 to $-\pi$. This works the same as the previous case, with the only difference being a clockwise rotation instead of counter clockwise. When $\psi = -\pi$,

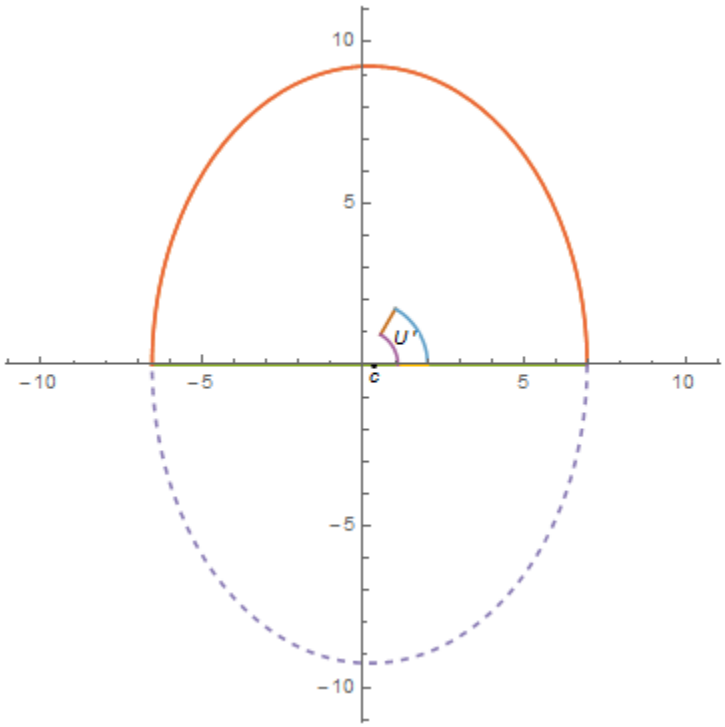

Figure 4.2: $\mathcal{E}$ with minor axis on $\mathbb{R}$, rotated counter-clockwise

U_a has been rotated by $-\frac{\pi}{2}$, so the minor axis of $\mathcal{E}$ lies on the real axis. The upper ray boundary of U_a' has argument 0 and the lower ray boundary of U_a' has argument $\geq -\frac{\pi}{3}$. See Figure 4.3.

Again, the argument of U_a' and U_a both change linearly so this is the first and only time that the boundary of U_a touches that of U_a'. Thus for $-\pi \leq \psi < 0$ we have $U_a' \subset U_a$. Thus we have shown that for $c \in \mathbb{R}$, $0 < c < t$, $|a| \leq 4$, $n \geq 3$, and $-\pi < \psi \leq \pi$, $U_a' \subset U_a$. □

We can combine this Proposition with facts established by Douady and Hubbard to make one further conclusion about these parameter values for which $U_a' \subset U_a$:

Theorem 4.3. *Let $n \geq 3$, $0 < c < t$, $|a| \leq 4$, and $\psi \neq \pi$. $R_{n,c,a}$ restricted to the set of points whose orbits remain in U_a' is topologically conjugate to some quadratic polynomial on its filled Julia set.*

Proof. We established in Proposition 4.2 that with these parameter restrictions we have

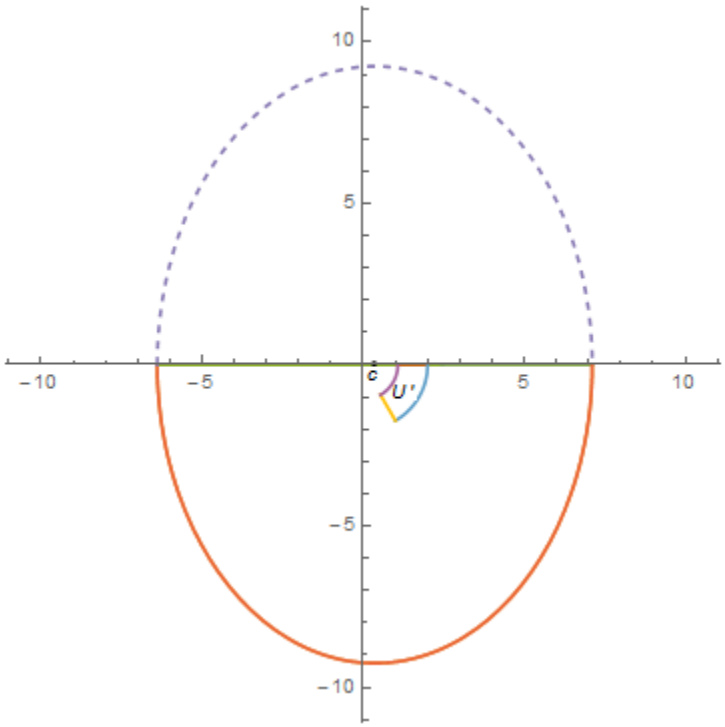

Figure 4.3: $\mathcal{E}$ with minor axis on $\mathbb{R}$, rotated clockwise

$U'_a \subset U_a$. We need the restriction that $\psi \neq \pi$ so that we can also claim that U'_a is also relatively compact in U_a for these restrictions. With this we can now say by Definition 2.1 that $R_{n,c,a}$ is a polynomial-like map of degree 2 on U'_a given these parameters. Thus, by Proposition 2.2, we have that the filled Julia set of $R_{n,c,a}$ on U'_a is topologically conjugate to the filled Julia set of some quadratic polynomial. □

Recall that the definition of the filled Julia set of a polynomial-like map consists of the collection of points in U'_a whose orbits never escape U'_a under iteration by $R_{n,c,a}$. This means that each U'_a set forward in this theorem must contain a portion of the whole filled Julia set of $R_{n,c,a}$ which is itself topologically conjugate to a filled Julia set of a quadratic polynomial. This means that there is some quadratic Julia set embedded in the Julia set of $R_{n,c,a}$. Figure 4.4a shows the filled Julia set of $R_{n,c,a}$ with $n = 3$, $c = 0.25$, and $a = 0.2$ along with the corresponding set $U'_{0.2}$. Next to it, Figure 4.4b shows the filled Julia set of the polynomial $P_{-1} = z^2 - 1$. We can see very clearly why we refer to these filled Julia sets inside U'_a as 'baby' quadratic Julia sets.

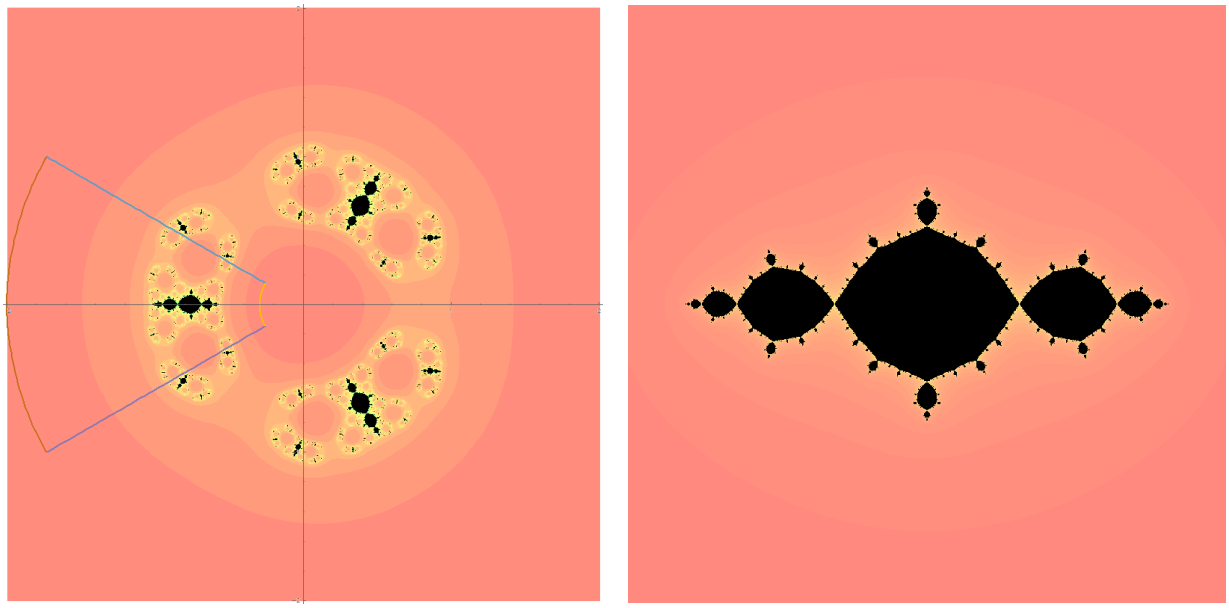

(a) U'_a overlaid on the filled Julia set of $R_{3,0.25,0.2}$ (b) The filled Julia set of $P_{-1} = z^2 - 1$

Figure 4.4: An example of one U'_a containing a baby Julia set juxtaposed alongside the filled Julia set of $z^2 - 1$

4.1.2 Results for $|c| > 1 + \epsilon$

For the next set of results in this chapter, we will find a boundedness locus when $|c| > 1+\epsilon$, where $\epsilon > 0$, for sufficiently large n. Once we have this locus we will use it to help show that $U'_a \subset U_a$. It is difficult to show this for all c-values $|c| > 1 + \epsilon$, so we will further restrict our parameters in order to show that $U'_a \subset U_a$.

To find the boundedness locus we first establish the locus for real values of c and then extend the result to complex values of c.

Proposition 4.4. *Given any $\epsilon > 0$, $c \in \mathbb{R}$, and $c > 1 + \epsilon$ there exists an $N \in \mathbb{N}$ such that for $n \geq N$ the boundedness locus of $R_{n,c,a}$ is contained in the polar rectangle L, where L is given by the set of a-values such that*

$$\frac{(c - (1+\epsilon))^2}{4} \leq |a| \leq \frac{(c + (1+\epsilon))^2}{4}$$

and

$$-2\sin^{-1}\left(\frac{1+\epsilon}{c}\right) \leq Arg(a) \leq 2\sin^{-1}\left(\frac{1+\epsilon}{c}\right).$$

Proof. From 2.4 we have that given any $c \in \mathbb{C}$, $a \in \mathbb{C}^*$, and given any $\epsilon > 0$ there is an $N \geq 2$ such that for all $n \geq N$, the filled Julia set of $R_{n,c,a}$ is contained in the disk of radius $1+\epsilon$ centered at 0. The assumptions that we have made satisfy these conditions, so in order for a to be in the boundedness locus for $R_{n,c,a}$, we must have at least one of $c \pm 2\sqrt{a}$ inside the disk of radius $1+\epsilon$.

Since $Re(2\sqrt{a}) > 0$, $c \in \mathbb{R}$ and $c > 1+\epsilon$ we have that $Re(c+2\sqrt{a}) > 1+\epsilon$, and so the orbit of $c+2\sqrt{a}$ cannot possibly remain bounded. Thus we can only look at $c-2\sqrt{a}$. Now, if $(c-2\sqrt{a}) \in \{z : |z| < 1+\epsilon\}$, then we must have $-2\sqrt{a} \in \{z : |z+c| < 1+\epsilon\}$. From this we get $\sqrt{a} \in \left\{z : |z - \frac{c}{2}| < \frac{1+\epsilon}{2}\right\}$. By squaring this region we can use the result to create a set of bounds for where the boundedness locus must occur. Since c is real and $c > 1+\epsilon$, this disk is centered on the real axis and $Re(z) > 0$ for all z inside it. Thus for all $\left\{z : |z - \frac{c}{2}| < \frac{1+\epsilon}{2}\right\}$, we get $\frac{c-(1+\epsilon)}{2} \leq |\sqrt{a}| \leq \frac{c+(1+\epsilon)}{2}$. When we square every point in this disk we end up with bounds for the modulus of a, given by

$$\frac{(c-(1+\epsilon))^2}{4} \leq |a| \leq \frac{(c+(1+\epsilon))^2}{4}.$$

We get the bounds for the argument of a by finding the largest and smallest arguments that occur on the disk of radius $\frac{1+\epsilon}{2}$ centered at $\frac{c}{2}$ and then doubling them. Since the disk is centered on the real axis, the largest and smallest arguments will simply be opposites of each other. The largest argument occurs when the line segment extending from the origin is tangent to our disk. We can use the right triangle this creates to find the angle. See Figure 4.5 for an illustration.

From this we see that the *sine* of this angle is $\frac{1+\epsilon}{c}$, so the largest argument is $\sin^{-1}(\frac{1+\epsilon}{c})$, and the smallest is $-\sin^{-1}(\frac{1+\epsilon}{c})$. Doubling these gives us the upper and lower bounds for

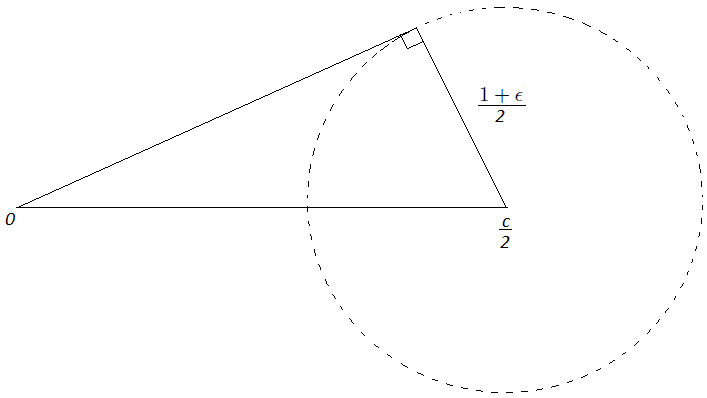

Figure 4.5: Illustration of the largest possible argument of a

the argument of a:

$$-2\sin^{-1}\left(\frac{1+\epsilon}{c}\right) \leq Arg(a) \leq 2\sin^{-1}\left(\frac{1+\epsilon}{c}\right).$$

So, for n sufficiently large, the modulus and argument of a must be bounded in both these ways in order for $c-2\sqrt{a}$ to be in the filled Julia set of $R_{n,c,a}$. Thus the boundedness locus for $R_{n,c,a}$ must be bounded the same way. □

We now complete the result for complex values of c by using a rotation argument.

Proposition 4.5. *Given any $\epsilon > 0$, $c \in \mathbb{C}$, and $|c| > 1+\epsilon$ there exists an $N \in \mathbb{N}$ such that for $n \geq N$ the boundedness locus of $R_{n,c,a}$ is contained in the polar rectangle L, where L is given by the set of a-values such that*

$$\frac{(|c|-(1+\epsilon))^2}{4} \leq |a| \leq \frac{(|c|+(1+\epsilon))^2}{4}$$

and

$$-2\sin^{-1}\left(\frac{1+\epsilon}{|c|}\right) + 2Arg(c) \leq Arg(a) \leq 2\sin^{-1}\left(\frac{1+\epsilon}{|c|}\right) + 2Arg(c).$$

Proof. The polar rectangle L here is simply the polar rectangle from Proposition 4.4, rotated by twice the argument of c. Suppose $|(|c|-2\sqrt{a})| < 1+\epsilon$. Then any rotation of $|c|-2\sqrt{a}$

will still satisfy the same inequality. Thus,

$$\begin{aligned}
\left|(|c| - 2\sqrt{a})\right| &< 1 + \epsilon \\
\left|(|c| - 2\sqrt{a})\right| \left|(e^{iArg(c)})\right| &< 1 + \epsilon \\
\left|(|c| - 2\sqrt{a})(e^{iArg(c)})\right| &< 1 + \epsilon \\
\left|(|c|e^{iArg(c)} - 2e^{iArg(c)}\sqrt{a}\right| &< 1 + \epsilon \\
\left|c - 2\sqrt{ae^{2iArg(c)}}\right| &< 1 + \epsilon.
\end{aligned}$$

We see that, if a is rotated by twice the argument of c, we get $c - 2\sqrt{a}$ within the disk of radius $1 + \epsilon$, and therefore this a is potentially in the boundedness locus. We can do this with any a from the polar rectangle from the previous Proposition, so we create the new polar rectangle by rotating the previous one by $2Arg(c)$. □

Now that we have found a region in which the boundedness locus lies, we can use this to help prove that $U'_a \subset U_a$. This polar rectangle L gives us a natural restriction for the values of a. We don't care if U'_a is contained in U_a for values of a outside of L, so we can restrict our a-values to those which lie within L. We again begin by showing that $U'_a \subset \mathcal{E}$.

Proposition 4.6. *Suppose we have $c \in \mathbb{C}$, $|c| > 1 + \epsilon$, $\epsilon > 0$, and a in the polar rectangle L from Proposition 4.5. There exists an $N \in \mathbb{N}$ sufficiently large such that the region U'_a associated with $R_{n,c,a}$ for any $n \geq N$ is contained in the ellipse $\mathcal{E}$.*

Proof. By Proposition 4.5, let N_1 be sufficiently large so that the boundedness locus of $R_{n,c,a}$ is contained in L. For a chosen c, let N_2 be large enough so that $6|c| + 4 < 2^{N_2+1}$. Finally, let $N = max\{N_1, N_2\}$. Now, for all $n \geq N$, we can use the inequalities $6|c| + 4 < 2^{n+1}$ and $|a| \leq \frac{(|c|+(1+\epsilon))^2}{4}$.

In order to show that U'_a is in $\mathcal{E}$ we will first show that U'_a is contained in the disk of

radius 2 centered at 0, and then that this disk is in $\mathcal{E}$. Recall the definition of U'_a:

$$U'_a = \left\{ z \;\middle|\; \frac{a^{\frac{1}{n}}}{2} < |z| < 2,\ \frac{\psi - \pi}{2n} < Arg(z) < \frac{\psi + \pi}{2n} \right\}.$$

By our assumptions we have

$$\begin{aligned} |a| &\leq \frac{(|c| + (1+\epsilon))^2}{4} \\ &< \frac{(|c| + |c|))^2}{4} \\ &= \frac{4|c|^2}{4} \\ &= |c|^2. \end{aligned}$$

Since $|c|^2 > |a|$ we can write $|c| > |a|^{1/2}$. From this we can create another inequality:

$$2^{n+1} > 6|c| + 4 > 6|c| > 2|c| > 2|a|^{1/2}.$$

If we manipulate $2|a|^{1/2} < 2^{n+1}$, we get

$$\begin{aligned} 2|a|^{1/2} &< 2^{n+1}, \\ |a|^{1/2} &< 2^n, \\ |a| &< 4^n, \\ |a|^{1/n} &< 4, \\ \frac{|a|^{1/n}}{2} &< 2. \end{aligned}$$

This verifies that our definition of U'_a works nicely for these a-values and shows that U'_a is in $\mathbb{D}(0,2)$. Next, to show that $\mathbb{D}(0,2)$ is in $\mathcal{E}$, we show that $|z - c + 2\sqrt{a}| + |z - c - 2\sqrt{a}| <$

$2^{n+1} + \frac{|a|}{2^{n-1}}$ for all $z \in \mathbb{D}(0,2)$. Let $|z| < 2$. Then,

$$\begin{aligned}
|z - c + 2\sqrt{a}| + |z - c - 2\sqrt{a}| &\leq 2|z| + 2|c| + 4|a|^{1/2} \\
&< 4 + 2|c| + 4|a|^{1/2} \\
&< 4 + 2|c| + 4|c| \\
&= 6|c| + 4 \\
&< 2^{n+1} \\
&< 2^{n+1} + \frac{|a|}{2^{n-1}}.
\end{aligned}$$

Thus for sufficiently large n we have U_a' contained in $\mathcal{E}$. □

We have shown that $U_a' \subset \mathcal{E}$ for these restrictions on a and c. Just as in Proposition 4.2 we can identify a simple case where $U_a' \cap U_a \neq \emptyset$, so again we can show that $U_a' \subset U_a$ by showing that U_a' does not intersect the minor axis of $\mathcal{E}$. Since $\mathcal{E}$ is centered at c, the position of $\mathcal{E}$ can vary greatly depending on c and it is difficult to ensure that the minor axis never touches U_a'. Therefore we put a couple of tighter restrictions on c in order to ensure that it never happens.

Proposition 4.7. *Suppose $c \in \mathbb{R}$, $c < 0$, $|c| > 1 + \epsilon$, and n sufficiently large so as to satisfy Proposition 4.6. Then for any $R_{n,c,a}$ with n, c, and a satisfying these conditions we have $U_a' \subset U_a$.*

Proof. By Proposition 4.6 we have that $U_a' \subset \mathcal{E}$. Once again we know that $a^{1/2n}$ maps to $c + 2\sqrt{a}$. Since c is real, if we select a positive real value for a then $\mathcal{E}$ is centered on the real axis with major axis along $\mathbb{R}$. As c is negative, we also have $c < a^{1/2n}$ for positive real a. Thus $U_a' \cap U_a \neq \emptyset$ for some a-value within our parameters. If we prove that the minor axis of $\mathcal{E}$ does not intersect U_a' for any n, c, and a with our restrictions, then once again we will

have $U'_a \subset U_a$. Recall the definition of U'_a:

$$U'_a = \left\{ z \;\middle|\; \frac{a^{\frac{1}{n}}}{2} < |z| < 2,\ \frac{\psi - \pi}{2n} < Arg(z) < \frac{\psi + \pi}{2n} \right\}.$$

Since $-\pi \leq \psi \leq \pi$ and $n \geq 3$, we have that $\frac{\psi+\pi}{2n} \leq \frac{2\pi}{2n} \leq \frac{\pi}{3}$ and $\frac{\psi-\pi}{2n} \geq -\frac{2\pi}{2n} \geq -\frac{\pi}{3}$. Thus for all $z \in U'_a$ we have $-\frac{\pi}{3} \leq arg(z) \leq \frac{\pi}{3}$.

Since c is real and negative, as $\mathcal{E}$ rotates based on a the first points where the minor axis potentially touches the polar rectangle $\frac{|a|^{1/n}}{2} \leq |z| \leq 2$, $-\frac{\pi}{3} \leq arg(z) \leq \frac{\pi}{3}$ will be at $2e^{\frac{\pi}{3}i}$ and $2e^{-\frac{\pi}{3}i}$, or $(1, \sqrt{3})$ and $(1, -\sqrt{3})$. To find at what angle of rotation this intersection occurs, we construct the triangle in Figure 4.6.

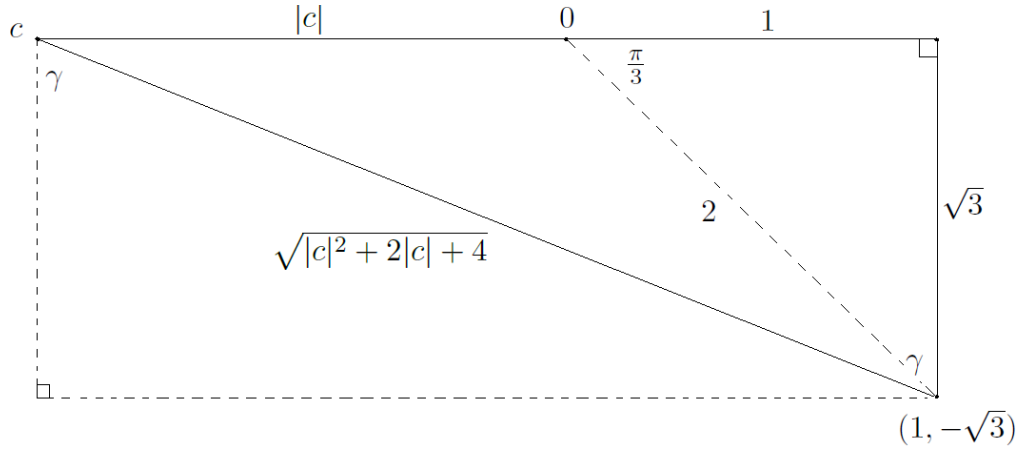

Figure 4.6: Finding the angle of the intersection

From this triangle we can determine that $\gamma = \sin^{-1}\left(\frac{|c|+1}{\sqrt{|c|^2+2|c|+4}}\right)$. Thus the minor axis of $\mathcal{E}$ intersects this polar region when the angle of rotation is $\sin^{-1}\left(\frac{|c|+1}{\sqrt{|c|^2+2|c|+4}}\right)$. The angle of rotation of $\mathcal{E}$ is given by $\frac{\psi}{2}$, so we shall show that given our restrictions we end up with $\frac{\psi}{2} < \sin^{-1}\left(\frac{|c|+1}{\sqrt{|c|^2+2|c|+4}}\right)$ for all allowable choices of n, c, and a.

Our restrictions on the argument of a say that

$$2arg(c) - \sin^{-1}\left(\frac{1+\epsilon}{|c|}\right) \leq \psi \leq 2arg(c) + \sin^{-1}\left(\frac{1+\epsilon}{|c|}\right).$$

Since $arg(c) = \pi$, this means that ψ is within $\sin^{-1}\left(\frac{1+\epsilon}{|c|}\right)$ of 2π, or 0. So we can say

$$-\sin^{-1}\left(\frac{1+\epsilon}{|c|}\right) \leq \psi \leq \sin^{-1}\left(\frac{1+\epsilon}{|c|}\right).$$

Thus by our restrictions we have

$$\frac{\psi}{2} \leq \frac{1}{2}\sin^{-1}\left(\frac{1+\epsilon}{|c|}\right) < \frac{1}{2}\sin^{-1}(1) = \frac{\pi}{4}.$$

Now we take a look at the contents of our other inverse sine.

$$\begin{aligned}\frac{|c|+1}{\sqrt{|c|^2+2|c|+4}} &= \frac{\sqrt{(|c|+1)^2}}{\sqrt{|c|^2+2|c|+4}} \\ &= \sqrt{\frac{|c|^2+2|c|+1}{|c|^2+2|c|+4}} \\ &= \sqrt{\frac{|c|^2+2|c|+4-3}{|c|^2+2|c|+4}} \\ &= \sqrt{1-\frac{3}{|c|^2+2|c|+4}}.\end{aligned}$$

Since $|c| > 1$, we have $|c|^2 + 2|c| + 4 > 7$, and so $\frac{1}{|c|^2+2|c|+4} < \frac{1}{7}$. Thus,

$$\frac{|c|+1}{\sqrt{|c|^2+2|c|+4}} = \sqrt{1-\frac{3}{|c|^2+2|c|+4}} > \sqrt{1-\frac{3}{7}} = \frac{2}{\sqrt{7}} > \frac{\sqrt{2}}{2}.$$

Since $\frac{|c|+1}{\sqrt{|c|^2+2|c|+4}} > \frac{\sqrt{2}}{2}$, we also have $\sin^{-1}\left(\frac{|c|+1}{\sqrt{|c|^2+2|c|+4}}\right) > \frac{\pi}{4}$. We have now shown that

$$\frac{\psi}{2} \leq \frac{1}{2}\sin^{-1}\left(\frac{1+\epsilon}{|c|}\right) < \frac{1}{2}\sin^{-1}(1) = \frac{\pi}{4} < \sin^{-1}\left(\frac{|c|+1}{\sqrt{|c|^2+2|c|+4}}\right).$$

A similar argument using an almost identical triangle gives us the following inequality:

$$\frac{\psi}{2} \geq -\frac{1}{2}\sin^{-1}\left(\frac{1+\epsilon}{|c|}\right) > -\frac{1}{2}\sin^{-1}(1) = -\frac{\pi}{4} > -\sin^{-1}\left(\frac{|c|+1}{\sqrt{|c|^2+2|c|+4}}\right).$$

From this we see that the minor axis of $\mathcal{E}$ never intersects the polar rectangle given by $\frac{|a|^{1/n}}{2} \leq |z| \leq 2$, $-\frac{\pi}{3} \leq arg(z) \leq \frac{\pi}{3}$ for any allowable choice of n, c, and a, and therefore never intersects U_a'. Thus we have $U_a' \subset U_a$ for $c \in \mathbb{R}$, $c < 0$, $|c| > 1+\epsilon$, and n sufficiently large. □

Just as with the small c case, we can now conclude that the sets U_a' with the above restrictions also contain baby Julia sets of quadratic polynomials.

Theorem 4.8. *Suppose $c \in \mathbb{R}$, $c < 0$, $|c| > 1+\epsilon$, where $\epsilon > 0$, and n sufficiently large so as to satisfy Proposition 4.6. Given these restrictions, $R_{n,c,a}$ restricted to the set of points whose orbits remain in U_a' is topologically conjugate to some quadratic polynomial on its filled Julia set.*

Proof. The proof for this theorem is the same as that of Theorem 4.3. The result follows from Proposition 2.2. □

4.2 Dynamics for Large c

In this section we constrain the parameter c so that we can go all the way and prove the existence of baby Mandelbrot sets in the parameter planes of $R_{n,c,a}$. We will show that, for $c \in \mathbb{C}$, $|c| \geq 6$ and n such that $4|c| + 8 \leq 2^{n+1}$, there exist n baby Mandelbrot sets in the boundedness locus of the a-parameter planes of the family of functions $R_{n,c,a}(z) = z^n + \frac{a}{z^n} + c$. Figure 4.7 shows two examples of these planes. We can see what look like n baby Mandelbrot sets present in each example. While this is a more narrow range of parameter values than we used in some of the results in the previous sections of this chapter, it still covers a very wide range of possible c-parameter values that can be chosen.

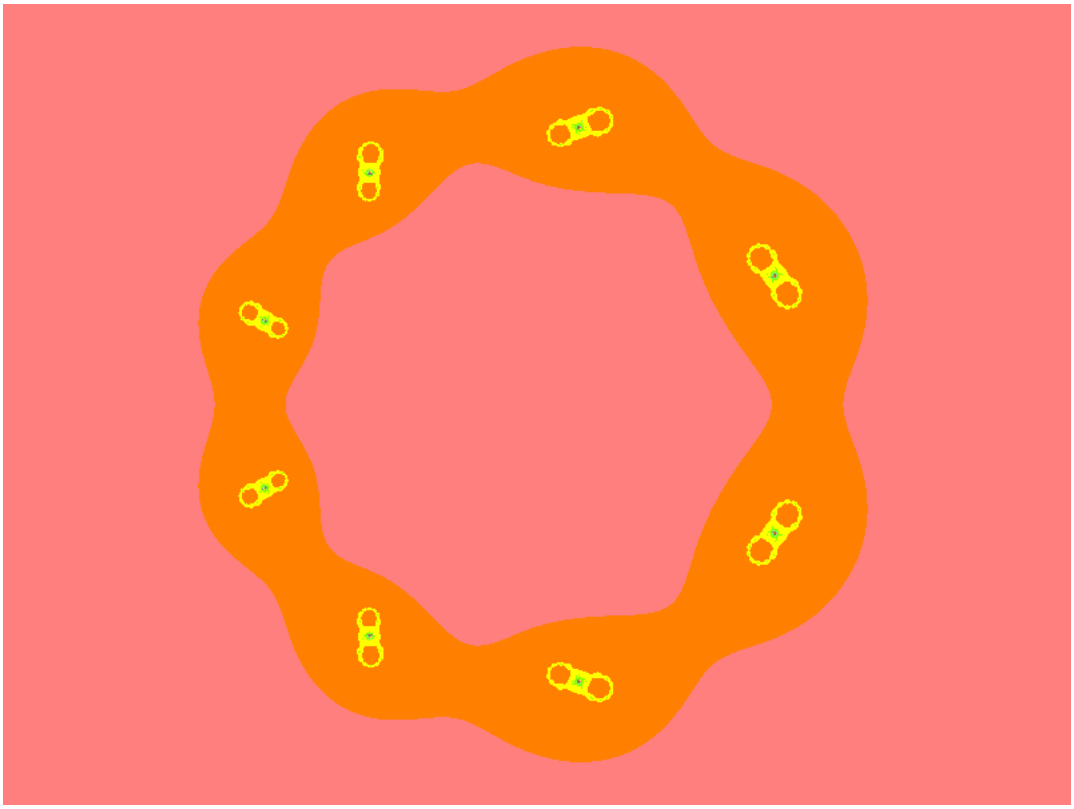

(a) a-plane for $n = 8$ and $c = 6$

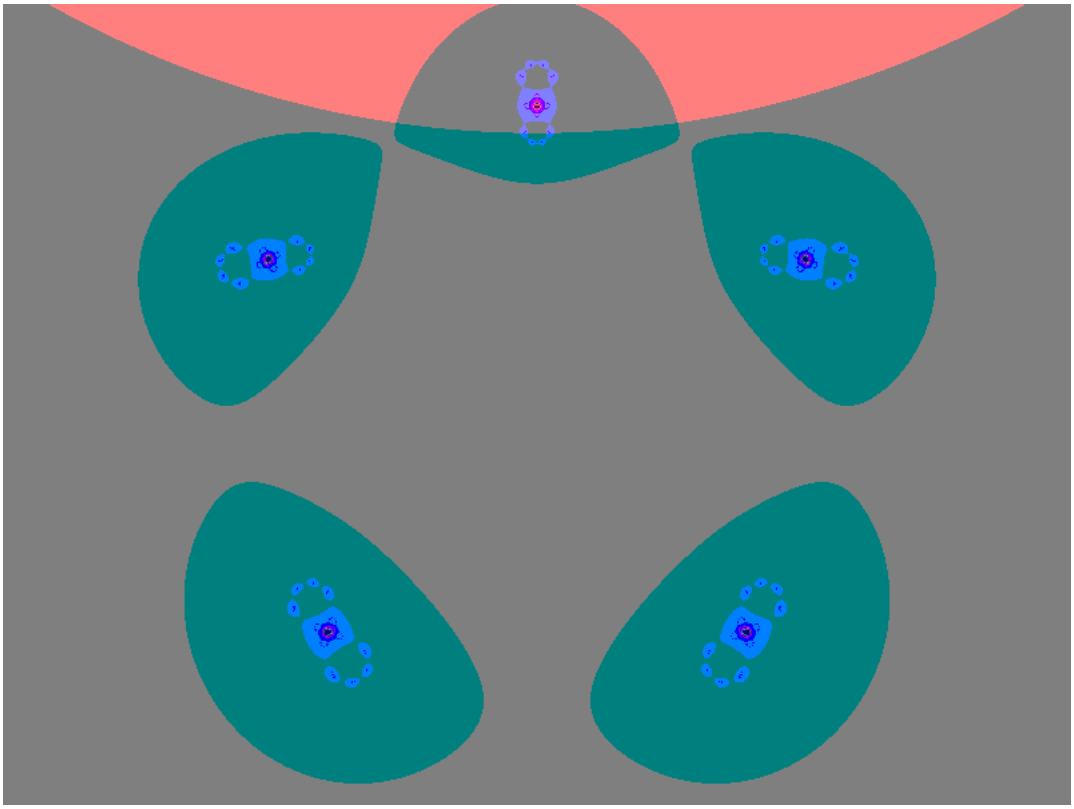

(b) a-plane for $n = 5$ and $c = -6 + 6i$

Figure 4.7: Two parameter planes of $R_{n,c,a}$

In Proposition 4.5 we established that for $|c| > 1 + \epsilon$ and sufficiently large n the boundedness locus of $R_{n,c,a}$ would be contained within the polar rectangle L. This essentially gives us a boundedness locus for our new parameter constraints, with only a small amount of tinkering required in some cases. Any $|c| \geq 6$ certainly falls within the range of $|c| > 1 + \epsilon$, so all we need is a sufficiently large N to force the boundedness locus inside L for any $n \geq N$. It is possible that there is an N which is sufficiently large so that $4|c| + 8 \leq 2^{n+1}$ for $n \geq N$ but which is not large enough to cause the boundedness locus to always fit inside L. In any such case it is a simple matter to use the larger of the two Ns so that we have both a concrete boundedness locus and proof of baby Mandelbrot sets.

The purpose of finding the 'spine' of a boundedness locus is to find a curve within the boundedness locus on which the centers of our primary baby Mandelbrot sets lie. This, in turn, allows to to better locate the potential baby Mandelbrot sets so that we can create appropriate U'_as to contain them. From Lemma 2.5 we have that given any $|c| > 1$, $n \geq 2$ there exist n solutions in the family of functions $R_{n,c,a}$ to the equation $c \pm 2\sqrt{a} = a^{1/2n}$. In other words, there are n fixed critical points in the a-plane. They are found by making the substitution $w^{2n} = a$ and solving $w^n = \frac{w}{2} - \frac{c}{2}$. This allows us to bypass finding a 'spine' for the boundedness locus, as we already know the number of potential principal baby Mandelbrots and can create our U'_as to surround these solutions.

Given $|c| \geq 6$ and a sufficiently large n we will show that for each of the n solutions, $w_1, w_2, ..., w_n$ there is a U'_a and a region in the a parameter plane, W_{c,w_j}, such that for all $a \in W_{c,w_j}$ we have $U'_a \subset R_{n,c,a}(U'_a) = U_a$. We will show that $R_{n,c,a} : U'_a \to U_a$ is polynomial-like of degree two on each W_{c,w_j}. We will show that for each a in the boundary of any W_{c,w_j} we have that the chosen fixed critical value $R_{n,c,a}(w_j) = c \pm 2\sqrt{a}$ is contained in $U_a - U'_a$. And lastly we will show that as a travels once around the boundary of any W_{c,w_j} the critical value $c \pm 2\sqrt{a}$ wraps once around the critical point $a^{1/2n}$. Hence by Theorem 2.3 we can conclude the existence of a baby Mandelbrot set within each W_{c,w_j}.

To begin we will first define a collection of regions in the a-plane with each corresponding

to one fixed critical point. Each of these regions is created so that they contain the entirety of one of our proposed baby Mandelbrot sets. They also act as constraints for our a-values, as we only need to consider values within the region to prove that it contains a baby Mandelbrot set.

Definition 4.9. *Given a family of functions $R_{n,c,a}$ with $|c| \geq 6$ and n sufficiently large so that $4|c| + 8 < 2^{n+1}$ there are n fixed critical points, $w_1, w_2, ..., w_n$. For each $w_1, ..., w_n$ we define W_{c,w_j} for $j \in 1, ..., n$ as the region in the a parameter plane bounded by the curves:*

$$\frac{1}{16}e^{2i\theta} - \frac{c}{4}e^{i\theta} + \frac{c^2}{4} \quad for \quad 0 \leq \theta \leq 2\pi \tag{4.1}$$

$$e^{2i\theta} - ce^{i\theta} + \frac{c^2}{4} \quad for \quad 0 \leq \theta \leq 2\pi \tag{4.2}$$

$$\frac{x^2}{4}e^{2i\left(Arg(w_j)-\frac{\pi}{2n}\right)} - \frac{xc}{2}e^{i\left(Arg(w_j)-\frac{\pi}{2n}\right)} + \frac{c^2}{4} \quad for \quad \frac{1}{2} \leq x \leq 2 \tag{4.3}$$

$$\frac{x^2}{4}e^{2i\left(Arg(w_j)+\frac{\pi}{2n}\right)} - \frac{xc}{2}e^{i\left(Arg(w_j)+\frac{\pi}{2n}\right)} + \frac{c^2}{4} \quad for \quad \frac{1}{2} \leq x \leq 2. \tag{4.4}$$

Curves (1) and (2) are found, respectively, by solving $|c + 2\sqrt{a}| = \frac{1}{2}$ and $|c + 2\sqrt{a}| = 2$ for a. Curves (3) and (4) are found, respectively, by solving $c + 2\sqrt{a} = xe^{i\left(Arg(w_j)-\frac{\pi}{2n}\right)}$ and $c + 2\sqrt{a} = xe^{i\left(Arg(w_j)+\frac{\pi}{2n}\right)}$ for a. We define W_{c,w_j} this way so that as the parameter a travels around the boundary of W_{c,w_j} the critical value $c + 2\sqrt{a}$ travels around a specific region. Curves (1) and (2) are both close to circular, while curves (3) and (4) are both arcs from arms of a parabola. Figures 4.8 and 4.9 give an idea of what a single W_{c,w_j} region looks like, as well as showing examples of the Ws containing the principal baby Mandelbrot sets.

The next step is to show that, for all a in each of the W_{c,w_j}, $R_{n,c,a}$ is polynomial-like of degree 2 on U'_a. To do this we will need to show that $U'_a \subset U_a$ for all valid choices of a.

Proposition 4.10. *The family of functions $R_{n,c,a}(z)$ is polynomial-like of degree 2 on each U'_a for a in any W_{c,w_j}. That is, $U'_a \subset U_a$ and $R_{n,c,a}$ maps U'_a two-to-one onto U_a.*

Proof. This proof will require several pieces to complete, so we'll take this step-by-step.

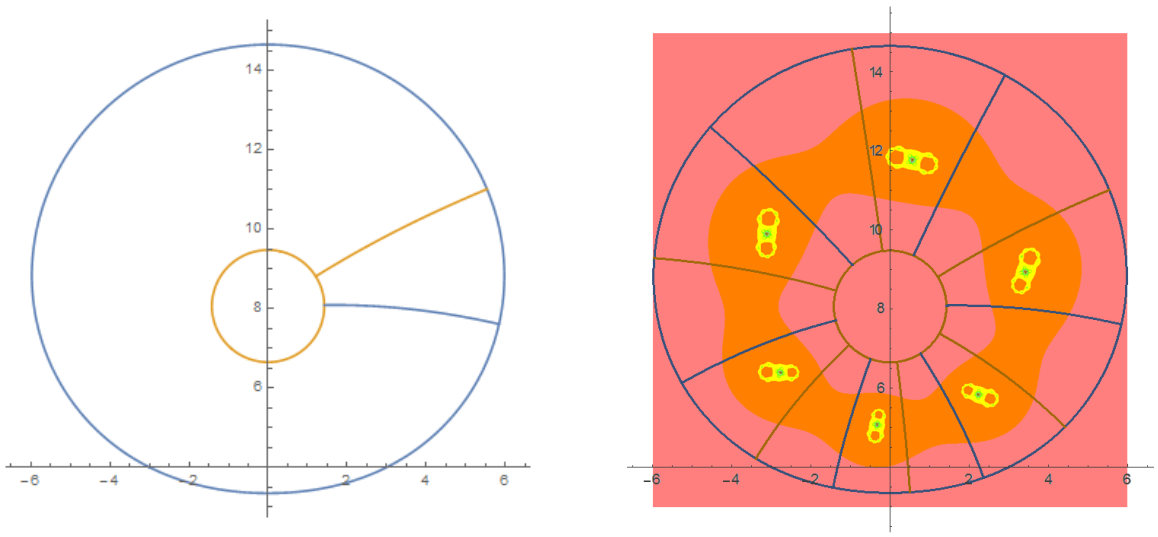

Figure 4.8: An example of one W_{c,w_j} for $c = 4 + 4i$ and $n = 6$ next to an overlay of all 6 of the W_{c,w_j} on top of the a parameter plane for $c = 4 + 4i$ and $n = 6$

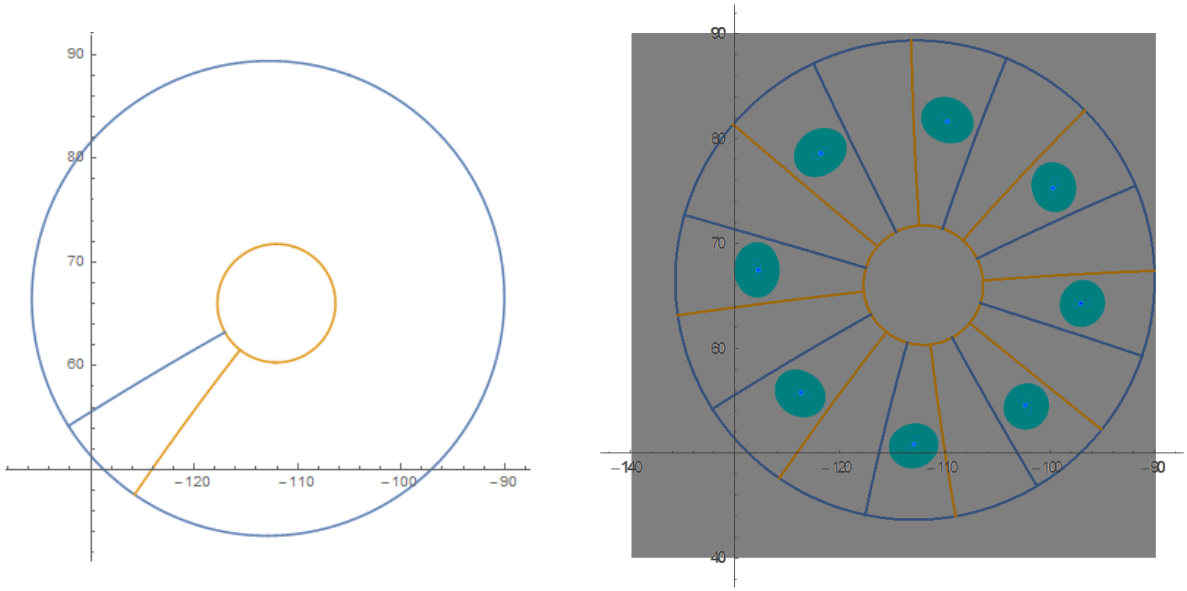

Figure 4.9: An example of one W_{c,w_j} for $c = -6 - 22i$ and $n = 8$ next to an overlay of all 6 of the W_{c,w_j} on top of the a parameter plane for $c = -6 - 22i$ and $n = 8$

First, recall the definition for U'_a:

$$U'_a = \left\{ z \;\middle|\; \frac{a^{\frac{1}{n}}}{2} < |z| < 2,\ \frac{\psi - \pi}{2n} < Arg(z) < \frac{\psi + \pi}{2n} \right\}.$$

The description of U_a in Lemma 3.3 also applies here as well, so we know that $R_{n,c,a}$ maps

U'_a two-to-one onto U_a. What we need to show to complete this proof is that $U'_a \subset U_a$ for every a in every W_{c,w_j}. As before, we will first establish that all of the U'_as are contained within the ellipse $\mathcal{E}$.

Lemma 4.11. *For any a in any W_{c,w_j}, $U'_a \subset \mathcal{E}$.*

Proof. To prove this we will show that the closed disk of radius 2 centered at 0 is contained in $\mathcal{E}$ and therefore so is U'_a. As specified in Lemma 3.3, the length of the semi-major axis of $\mathcal{E}$ is given by $2^n + \frac{|a|}{2^n}$ and the length of the semi-minor axis of $\mathcal{E}$ is given by $2^n - \frac{|a|}{2^n}$. A simple calculation shows us that the distance from the center of the ellipse to the foci is $2\sqrt{|a|}$. Recall that $\mathcal{E}$ is centered at c and is rotated by a degree of $\frac{\psi}{2}$. This means that the two foci of $\mathcal{E}$ occur at $c \pm 2\sqrt{a}$, which are also the two critical values for $R_{n,c,a}$.

Now that we know the locations of the two foci of $\mathcal{E}$ we can prove that $\overline{\mathbb{D}}_2(0)$ is contained in $\mathcal{E}$ by examining the sum $|z - (c + 2\sqrt{a})| + |z - (c - 2\sqrt{a})|$ for $|z| \leq 2$. The sum of the distances from any point on $\mathcal{E}$ to each foci is $2\left(2^n + \frac{|a|}{2^n}\right)$. If we can show that $|z - (c + 2\sqrt{a})| + |z - (c - 2\sqrt{a})| < 2\left(2^n + \frac{|a|}{2^n}\right)$ for all allowable choices of a then this would give us that $\overline{\mathbb{D}}_2(0) \subset \mathcal{E}$. To do this we will first find an upper bound for the magnitude of a. Recall that for each W_{c,w_j} the outer boundary is given by

$$e^{2i\theta} - ce^{i\theta} + \frac{c^2}{4} \text{ for } 0 \leq \theta \leq 2\pi.$$

From this we can say that

$$\begin{aligned} |a| &\leq \left| e^{2i\theta} - ce^{i\theta} + \frac{c^2}{4} \right| \\ &\leq |e^{2i\theta}| + |ce^{i\theta}| + \left| \frac{c^2}{4} \right| \\ &= \frac{|c|^2}{4} + |c| + 1 \\ &= \left(\frac{|c|}{2} + 1 \right)^2. \end{aligned}$$

Going back to $|z-(c+2\sqrt{a})|+|z-(c-2\sqrt{a})|$ and using our initial assumption that n is sufficiently large so that $4|c|+8 \leq 2^{n+1}$ we now have

$$\begin{aligned}
|z-(c+2\sqrt{a})|+|z-(c-2\sqrt{a})| &\leq 2|z|+2|c|+4|a|^{1/2} \\
&\leq 4+2|c|+4\left(\frac{|c|}{2}+1\right) \\
&= 4|c|+8 \\
&\leq 2^{n+1} \\
&< 2^{n+1}+\frac{|a|}{2^{n-1}} \\
&= 2\left(2^n+\frac{|a|}{2^n}\right).
\end{aligned}$$

Thus $\overline{\mathbb{D}}_2(0) \subset \mathcal{E}$ and therefore $U_a' \subset \mathcal{E}$. □

The next step requires us to show that U_a' does not touch the minor axis of $\mathcal{E}$ so that we can say that $U_a' \subset U_a$. This has been difficult in the past and has often required us to alter our parameters in order to show that it is true. With the parameters that we have chosen this time we will not need to alter anything. However, we do need to establish one property about the argument of a in order to prove definitively that $U_a' \subset U_a$ for our chosen parameters.

Lemma 4.12. *As a varies throughout any given W_{c,w_j}, the argument of $a^{1/2n}$ changes by less than $\frac{\pi}{2n}$.*

Proof. We mentioned earlier that as we trace a around the boundary of a given W_{c,w_j} the associated critical value travels around a specific region. We will call this region V_{c,w_j} and define

$$V_{c,w_j} = \left\{ z \;\middle|\; \frac{1}{2} \leq |z| \leq 2,\ arg(w_j) - \frac{\pi}{2n} \leq arg(z) \leq arg(w_j) + \frac{\pi}{2n} \right\}.$$

The two ray boundaries of V_{c,w_j} are created when a is on the two boundary curves of W_{c,w_j} given by

$$\frac{r^2}{4}e^{2i(arg(w_j)+\frac{\pi}{2n})} - \frac{rc}{2}e^{i(arg(w_j)+\frac{\pi}{2n})} + \frac{c^2}{4} \quad for \quad \frac{1}{2} \leq r \leq 2$$

and

$$\frac{r^2}{4}e^{2i(arg(w_j)-\frac{\pi}{2n})} - \frac{rc}{2}e^{i(arg(w_j)-\frac{\pi}{2n})} + \frac{c^2}{4} \quad for \quad \frac{1}{2} \leq r \leq 2.$$

First we show that for any fixed r in $\frac{1}{2} \leq r \leq 2$, the change in argument of

$$\frac{r^2}{4}e^{2i(arg(w_j)+x)} - \frac{rc}{2}e^{i(arg(w_j)+x)} + \frac{c^2}{4}$$

as $x : -\frac{\pi}{2n} \to \frac{\pi}{2n}$ is less than $\frac{2\pi}{n}$.

Notice that we can write

$$\frac{r^2}{4}e^{2i(arg(w_j)+x)} - \frac{rc}{2}e^{i(arg(w_j)+x)} + \frac{c^2}{4} = \left(\frac{r}{2}e^{i(arg(w_j)+x)} - \frac{c}{2}\right)^2.$$

If we use the fact that $arg(re^{i(\theta+x)} + se^{i\psi}) < arg(re^{i\theta} + se^{i\psi}) + x$ when $r \neq 0$ and $s \neq 0$, we see that as $x : -\frac{\pi}{2n} \to \frac{\pi}{2n}$, $arg\left(\frac{r}{2}e^{i(arg(w_j)+x)} - \frac{c}{2}\right)$ changes by less than $2(\frac{\pi}{2n}) = \frac{\pi}{n}$. Thus, as $x : -\frac{\pi}{2n} \to \frac{\pi}{2n}$, $arg\left(\frac{r}{2}e^{i(arg(w_j)+x)} - \frac{c}{2}\right)^2$ changes by less than $\frac{2\pi}{n}$. So, in crossing over W_{c,w_j} from one parabolic arc to another gives a change in argument of less than $\frac{2\pi}{n}$. If $arg(a)$ changes by less than $\frac{2\pi}{n}$, then $arg(a^{1/2n})$ changes by less than $\frac{\pi}{n^2}$. Since $n \geq 3$ we can write this as $\frac{\pi}{n^2} \leq \frac{\pi}{3n}$.

Next, the two inner and outer boundaries of V_{c,w_j} are created when a is on the two boundary curves of W_{c,w_j} given by

$$\frac{1}{16}e^{2i\theta} - \frac{c}{4}e^{i\theta} + \frac{c^2}{4} \quad for \quad 0 \leq \theta \leq 2\pi$$

and

$$e^{2i\theta} - ce^{i\theta} + \frac{c^2}{4} \quad for \quad 0 \leq \theta \leq 2\pi.$$

Here we will show that, for fixed θ, the change in argument of a as we go from the inner to the outer bound is less than $\frac{\pi}{6}$. Once again notice that we can write

$$\frac{1}{16}e^{2i\theta} - \frac{c}{4}e^{i\theta} + \frac{c^2}{4} = \left(\frac{e^{i\theta}}{4} - \frac{c}{2}\right)^2$$

and

$$e^{2i\theta} - ce^{i\theta} + \frac{c^2}{4} = \left(e^{i\theta} - \frac{c}{2}\right)^2.$$

Since c and θ are fixed we can think of $\left(re^{i\theta} - \frac{c}{2}\right)$ as a triangle in $\mathbb{C}$ and examine what happens to the argument as we take $r : \frac{1}{4} \to 1$. The change in argument for $\left(re^{i\theta} - \frac{c}{2}\right)$ as $r : \frac{1}{4} \to 1$ will be greatest when $\theta = arg(c) \pm \frac{\pi}{2}$. We have assumed $|c| \geq 6$, so $\frac{|c|}{2} \geq 3$ and we have a right triangle where the shortest leg is increasing in length from $\frac{1}{4}$ to 1. Since $\frac{|c|}{2} \geq 3$ we have $arg\left(\frac{e^{i\theta}}{4} - \frac{c}{2}\right) \leq \tan^{-1}(\frac{1}{12})$ and $arg\left(e^{i\theta} - \frac{c}{2}\right) \leq \tan^{-1}(\frac{1}{3})$. The change in argument will be greater the smaller $|c|$ is, so the change in argument for $\left(re^{i\theta} - \frac{c}{2}\right)$ as $r : \frac{1}{4} \to 1$ is less than or equal to $\tan^{-1}(\frac{1}{3}) - \tan^{-1}(\frac{1}{12}) < \frac{\pi}{12}$.

The change in argument for $\left(re^{i\theta} - \frac{c}{2}\right)$ as $r : \frac{1}{4} \to 1$ is less than $\frac{\pi}{12}$, so the change in argument for $\left(re^{i\theta} - \frac{c}{2}\right)^2$ as $r : \frac{1}{4} \to 1$ is less than $\frac{\pi}{6}$. If $arg(a)$ changes by less than $\frac{\pi}{6}$, then $arg(a^{1/2n})$ changes by less than $\frac{\pi}{12n}$.

As a travels from any point in a given W_{c,w_j} to another, we can think of this change as a shift along two arcs, one of each of the two types detailed above. Therefore we can say that the change in argument of $a^{1/2n}$ as a travels from any one point in W_{c,w_j} to another is less than $\frac{\pi}{n^2} + \frac{\pi}{12n}$. From here we see that

$$\frac{\pi}{n^2} + \frac{\pi}{12n} \leq \frac{\pi}{3n} + \frac{\pi}{12n} = \frac{5\pi}{12n} < \frac{6\pi}{12n} = \frac{\pi}{2n},$$

so as a varies throughout any given W_{c,w_j} the argument of $a^{1/2n}$ changes by less than $\frac{\pi}{2n}$. $\square$

This Lemma gives us the ability to show that $U'_a \subset U_a$, so that will be the next thing that we do.

Lemma 4.13. *For any a in any W_{c,w_j}, $U'_a \subset U_a$.*

Proof. We have already shown that for any a in one of the W_{c,w_j} the set U'_a is contained in $\mathcal{E}$. Since U'_a varies analytically as a varies and there exists an a in each W_{c,w_j} such that $a^{1/2n} \in U'_a$ is fixed, all that needs to be shown is that U'_a never intersects the minor axis of $\mathcal{E}$. To do this we will show that a disk of radius $2\sqrt{|a|}$ centered at $c \pm 2\sqrt{a}$ contains U'_a.

In each W_{c,w_j} there is an a such that $a^{1/2n} = c \pm 2\sqrt{a}$. At this a-value U'_a is contained almost exactly by the region traced out by the critical value as a travels around the boundary of W_{c,w_j}. The only difference is that the inner arc boundary of U'_a has magnitude $\frac{|a|^{1/n}}{2}$ while the inner arc that the critical value traces has magnitude $\frac{1}{2}$. Recall from the definition of W_{c,w_j} that the outer boundary of W_{c,w_j} is given by $e^{2i\theta} + ce^{i\theta} + \frac{c^2}{4}$ and note that therefore

$$\begin{aligned} |a| &\geq \left|\frac{c^2}{4}\right| - |ce^{i\theta}| - |e^{2i\theta}| \\ &= \frac{|c|^2}{4} - |c| - 1 \\ &\geq \frac{(6)^2}{4} - 7 \\ &= 2. \end{aligned}$$

Thus $|a| > 1$, and so $\frac{1}{2} < \frac{|a|^{1/n}}{2}$.

We showed in Lemma 4.12 that as a varies in W_{c,w_j} the argument of $a^{1/2n}$ can change by no more than $\frac{\pi}{2n}$. The radius of the smallest circle centered at $c \pm 2\sqrt{a}$ that is guaranteed to contain U'_a for any a in W_{c,w_j} is found using the triangle in Figure 4.10. The difference in argument between $c \pm 2\sqrt{a}$ and the furthest corner of U'_a is no more than $\frac{3\pi}{2n}$ and since $n \geq 3$ we get $\frac{3\pi}{2n} \leq \frac{\pi}{2}$. This means that one of the short legs of the triangle, labeled x, has length less than or equal to $\frac{\sqrt{2}}{2}$. The other short leg has length $\frac{3}{2}$. From this we get that the radius of the smallest circle at $c \pm 2\sqrt{a}$ that is guaranteed to contain U'_a is less than or equal to $\frac{3+\sqrt{2}}{2}$.

Now, $|a| \geq 2$, so $2\sqrt{|a|} \geq 2\sqrt{2}$, which is greater than $\frac{3+\sqrt{2}}{2}$. Thus for any $a \in W_{c,w_j}$ a

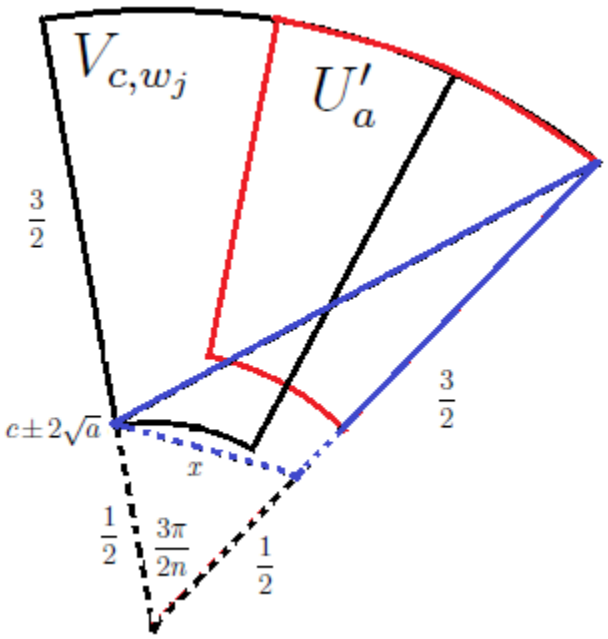

Figure 4.10: Finding the smallest circle which contains U'_a

disk of radius $2\sqrt{|a|}$ centered at the critical value will contain U'_a. This guarantees us that $U'_a \subset U_a$. □

Now we can say that $U'_a \subset U_a$ and U'_a is relatively compact in U_a for any choice of a in any of the W_{c,w_j}. This combined with the fact that $R_{n,c,a}$ is a proper analytic map which maps U'_a two-to-one onto U_a gives us that $R_{n,c,a}$ is a polynomial-like map of degree 2 on each U'_a for any a in any W_{c,w_j}. □

So far we have satisfied the first four conditions in Theorem 2.3 set forth by Douady and Hubbard to show that we have a homeomorphic copy of the Mandelbrot set:

(1) Each W_{c,w_j} is a closed disk contained in an open set in $\mathbb{C}$.

(2) By our definitions, the boundaries of U'_a and U_a both vary analytically as a varies.

(3) The map $(a, z) \mapsto R_{n,c,a}(z)$ depends analytically on both a and z.

(4) On each W_{c,w_j}, $R_{n,c,a}$ has a unique critical point and is polynomial-like of degree 2.

All that is left to show is that as a winds once around the boundary of any W_{c,w_j} the critical value winds once around the critical point. If we can show this last thing then we will have

shown that for each one of our W_{c,w_j} there is a corresponding baby copy of the Mandelbrot set.

Lemma 4.14. *On each region W_{c,w_j} the corresponding function given by $R_{n,c,a}$ has a unique critical point. As we trace the parameter a once around the boundary of any W_{c,w_j}, the image of this unique critical point winds once around the critical point itself.*

Proof. As mentioned in Lemma 4.12, as a winds once around the boundary of any W_{c,w_j} the critical value, $c \pm 2\sqrt{a}$, winds once around the boundary of

$$V_{c,w_j} = \left\{ z \;\middle|\; \frac{1}{2} \leq |z| \leq 2 \;\;,\;\; arg(w_j) - \frac{\pi}{2n} \leq arg(z) \leq arg(w_j) + \frac{\pi}{2n} \right\}.$$

Recall that each region W_{c,w_j} contains a parameter value for which the critical point, $a^{1/2n}$, is fixed. We refer to this fixed critical point as w_j and the set V_{c,w_j} is centered around this point. The argument of $c \pm 2\sqrt{a}$ changes more rapidly than the argument of $a^{1/2n}$ as a varies away from the parameter value corresponding with w_j. Since $c \pm 2\sqrt{a}$ traverses the boundary of V_{c,w_j}, this means that $a^{1/2n}$ must remain within the interior of V_{c,w_j} for all $a \in W_{c,w_j}$. Thus as a winds once around the boundary of any W_{c,w_j}, the critical value winds once around the critical point. □

Combining Proposition 4.10 with the previous Lemma gives us the result we are looking for.

Theorem 4.15. *For $|c| \geq 6$ and n sufficiently large so that $4|c| + 8 \leq 2^{n+1}$, there exist n 'primary' homeomorphic copies of the Mandelbrot set in the boundedness locus in the a-plane of the family of functions $R_{n,c,a}(z) = z^n + \frac{a}{z^n} + c$.*

Proof. Proposition 4.10 gives us that $R_{n,c,a}$ is polynomial-like of degree 2 on each W_{c,w_j}. This combined with Lemma 4.14 finishes our proof. For each $j \in 1, 2, ..., n$ the set of all a in the set W_{c,w_j} for which the orbit of the critical point $a^{1/2n}$ does not escape from U'_a is homeomorphic to the Mandelbrot set. There are n such fixed critical points and n such

regions so there must exist at least n homeomorphic copies of the Mandelbrot set within the a-parameter planes of $R_{n,c,a}$. □

Chapter 5

Investigating Other Slices of the (c, a) Parameter Plane

We have shown that baby Mandelbrot sets exist in the a-parameter plane for $R_{n,c,a}$ given certain parameter restrictions. The full range of (c, a) values is a two-complex dimensional parameter space. By fixing c and drawing the a-plane we are able to examine vertical slices of the (c, a) parameter space. We will now investigate other one-dimensional slices of the (c, a) space.

With $R_{n,c,a}$ we would fix c and n and then examine the behavior of the a-plane, so while there were 3 different parameters only one of them varied. What we would like to do is to look at a variation of $R_{n,c,a}$ where both the 'a' and 'c' parameters change. Having them both vary independently of each other is a bit problematic, as we would then have to visualize a 4-dimensional space to get a full idea of the dynamics going on. So, instead, we will set c so that it varies along with a, but in a fashion where one depends on the other. What we are looking for will stay the same: a boundedness locus, a 'spine' for the boundedness locus, solutions to $c \pm 2\sqrt{a} = a^{1/2n}$, and proof of the existence of baby Mandelbrot sets. In this chapter we will find both a 'spine' and a boundedness locus in these new slices. The family

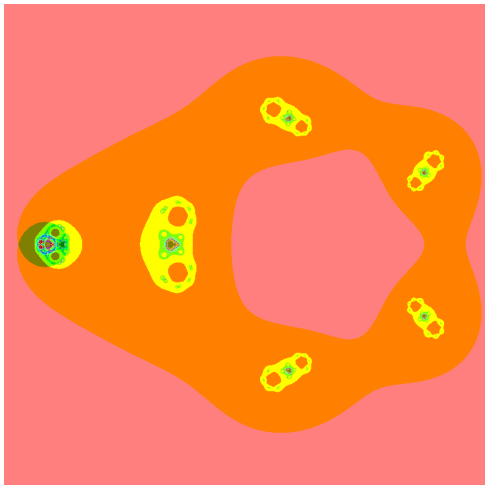

(a) $t = 0.8$

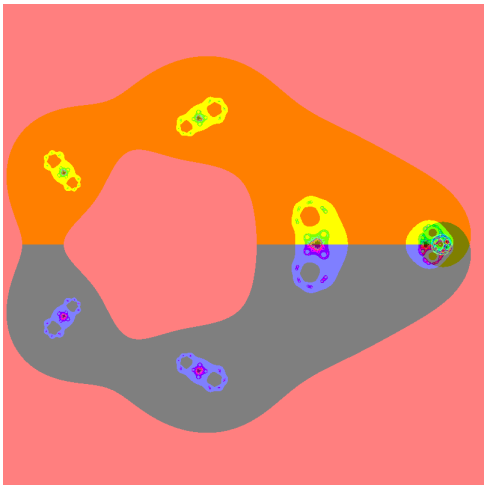

(b) $t = -0.8i$

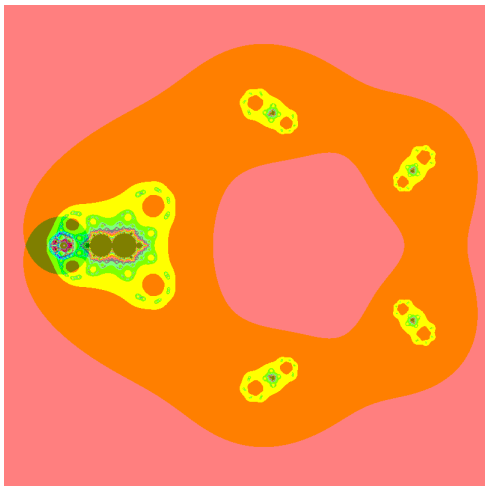

(c) $t = 1$

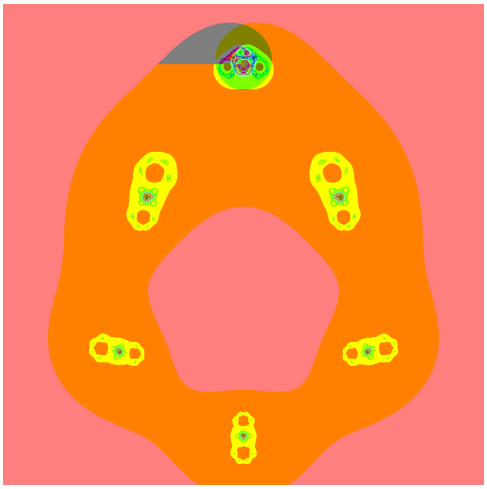

(d) $t = \frac{\sqrt{2}}{2} + i\frac{\sqrt{2}}{2}$

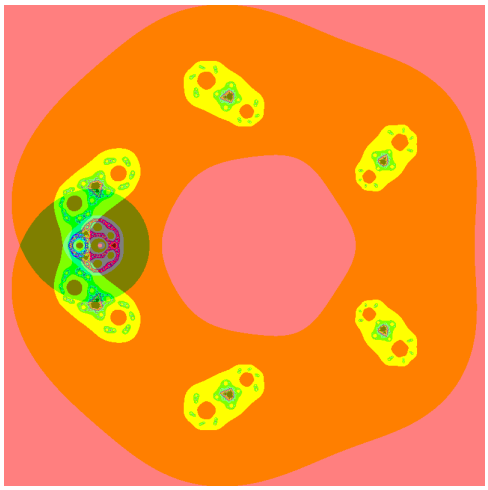

(e) $t = 2$

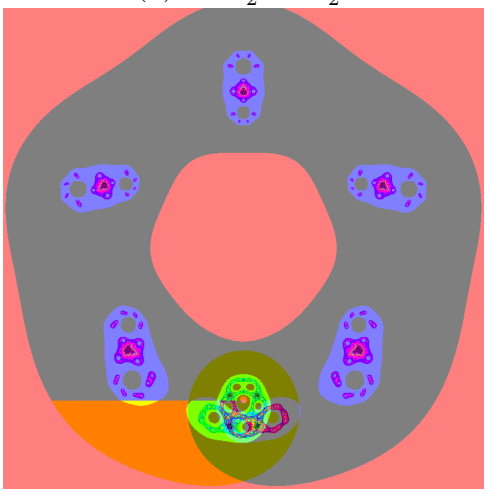

(f) $t = -\sqrt{2} + i\sqrt{2}$

Figure 5.1: Parameter planes of $R_{5,t,a}$

of functions that we will investigate is the family of rational functions

$$R_{n,ta,a}(z) = z^n + \frac{a}{z^n} + ta,$$

where $n \geq 3$, $a \in \mathbb{C} \setminus \{0\}$, and $t \in \mathbb{C} \setminus \{0\}$. Here we have taken the rational family $R_{n,c,a}$ and modified it so that instead of c being a fixed complex number we set $c = ta$ where t is complex. To study a member of this family we will fix an n, fix a t, and allow a to vary analytically. With this setup the parameter c no longer remains constant, instead varying as we move through the a-plane. With this change we will now be examining all linear slices through the origin in the (c, a) parameter space. Figure 5.1 shows a few examples of a-planes for various values of t when $n = 5$. We see again what appear to be small copies of the Mandelbrot set in these parameter planes. Figure 5.2 shows a zoomed-in example of one such set.

5.1 The Spines of $R_{n,ta,a}$

For this parameterization of the family the first thing we are going to find is the 'spine' of the boundedness locus. Finding the boundedness locus is not as straightforward as it has been for certain members of $R_{n,c,a}$, so for $R_{n,ta,a}$ we are going to create a boundedness locus by first finding a 'spine' and then building the locus up around it.

This reparameterization of the family of functions from $R_{n,c,a}$ to $R_{n,ta,a}$ does not affect the location of the Julia sets for $R_{n,ta,a}$. Once we've fixed an a and c (which gets fixed when a does), we get a Julia set. We saw in Corollary 2.4 from [BS11] that Julia sets for $R_{n,c,a}$ are near the unit circle, and that is still the case. This Corollary states that for any $c \in \mathbb{C}$ and $a \in \mathbb{C}^*$, given any $\epsilon > 0$, there is an $N \geq 2$ such that for all $n > N$, the filled Julia set is contained within an ϵ-annulus of the unit circle. The proofs for the Lemmas which this Corollary draws upon do not change when we fix a complex number t and replace c with ta. This means that even with this modification to the family of rational functions the filled

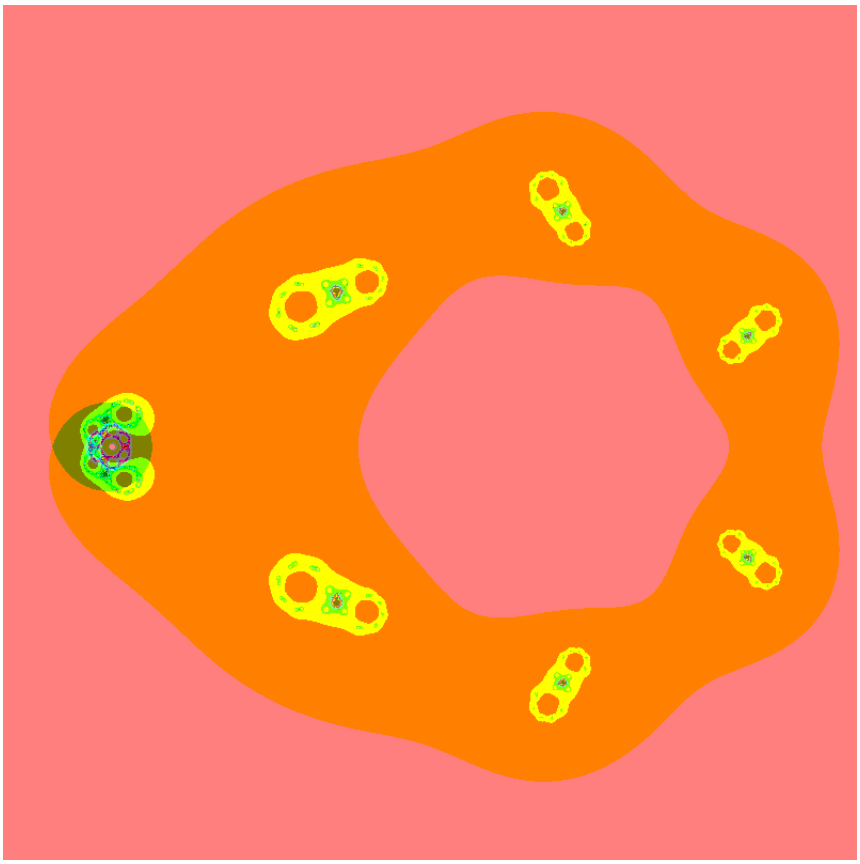

(a) Parameter plane for $n = 6$

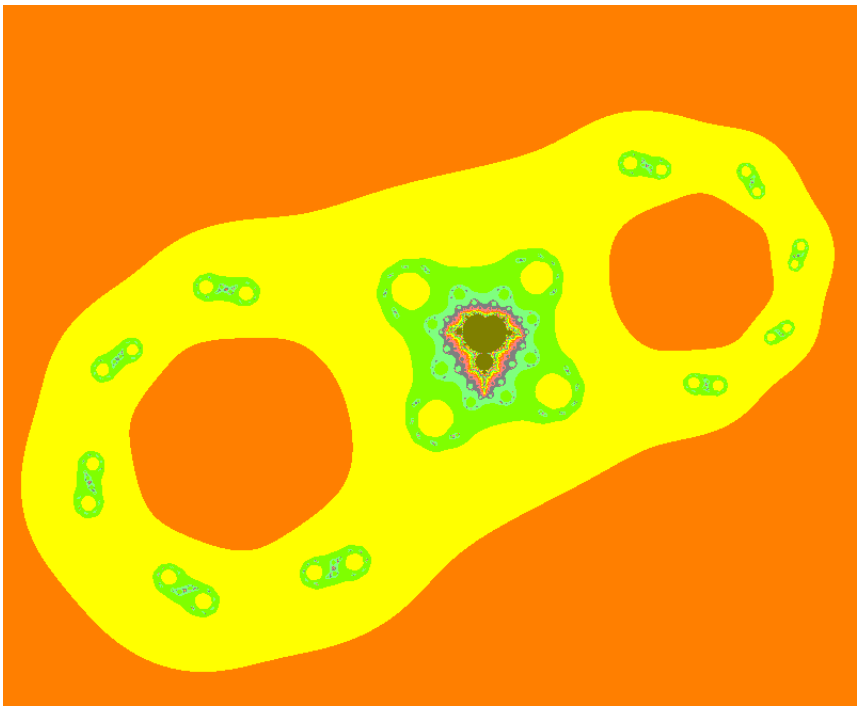

(b) Zoomed in view

Figure 5.2: $R_{n,ta,a}(z) = z^n + \frac{a}{z^n} + ta$ with $n = 6$ and $t = 1$

Julia sets of this new family still fall within the annulus $\mathbb{A}(1-\epsilon, 1+\epsilon)$ when n is sufficiently large.

We denote $M_n(R_{n,ta,a}) = \{a \in \mathbb{C} |$ at least one free critical orbit of $R_{n,ta,a}$ is bounded$\}$ and begin to describe the region in which this boundedness locus must lie by finding a curve around which it is centered. Our strategy is as follows: since the Julia sets must be near the unit circle, bounded critical orbits must be near the unit circle as well.

Proposition 5.1. *For any $t \in \mathbb{C} \setminus \{0\}$, the set of all $a \in \mathbb{C}$ for which at least one of the equations $|ta + 2\sqrt{a}| = 1$ or $|ta - 2\sqrt{a}| = 1$ holds true is given by the set*

$$\mathcal{S}_t = \left\{ a = \frac{2}{t^2} + \frac{1}{t}e^{i\theta} \pm \frac{2}{t^2}\sqrt{1 + te^{i\theta}} \;\middle|\; 0 \leq \theta \leq 2\pi \right\}.$$

We will refer to these curves as the 'spines' of the boundedness loci of $R_{n,ta,a}$, on which the baby Mandelbrot sets lie.

Proof. We can write $|ta \pm 2\sqrt{a}| = 1$ as $ta \pm 2\sqrt{a} = e^{i\theta}$ for some θ. To solve this for a we perform a substitution and use the quadratic equation.
The solutions to $tu^2 \pm 2u - e^{i\theta} = 0$ are given by

$$u = \frac{\mp 1 \pm \sqrt{1 + te^{i\theta}}}{t},$$

so the solutions to $ta \pm 2\sqrt{a} - e^{i\theta} = 0$ are given by

$$a = \left(\frac{\mp 1 \pm \sqrt{1 + te^{i\theta}}}{t} \right)^2 = \frac{2}{t^2} + \frac{1}{t}e^{i\theta} \pm \frac{2}{t^2}\sqrt{1 + te^{i\theta}}.$$

Thus, the collection of a-values for which $|ta \pm 2\sqrt{a}| = 1$ is

$$\left\{ \frac{2}{t^2} + \frac{1}{t}e^{i\theta} \pm \frac{2}{t^2}\sqrt{1 + te^{i\theta}} \;\middle|\; 0 \leq \theta \leq 2\pi \right\}.$$

□

Figure 5.3 shows three of these curves alongside their corresponding a-planes. Notice that when $t = 1$ we get a bifurcation, where values of t less than one give a spine which has split into two disconnected curves.

5.2 The Boundedness Locus of $R_{n,ta,a}$

Now we will find a region which contains the boundedness locus for $R_{n,ta,a}$ with the only condition being that n is sufficiently large. We will create this region by taking our spine, $\mathcal{S}_t$, and showing that the boundedness locus must lie within an ϵ-neighborhood of $\mathcal{S}_t$. In order to show that $M_n(R_{n,ta,a})$ must lie within a neighborhood of $\mathcal{S}_t$, we first restrict it to an annulus based on $|t|$. Denote

$$u(t) = \frac{2}{|t|^2} + \frac{1}{|t|} + \frac{2}{|t|^2}\sqrt{1+|t|}$$

and

$$l(t) = \frac{2}{|t|^2} + \frac{1}{|t|} - \frac{2}{|t|^2}\sqrt{1+|t|}.$$

Lemma 5.2. *Let $\epsilon > 0$, $t \in \mathbb{C} \setminus \{0\}$. There exists an $N \geq 2$ such that for all $n \geq N$ we have*

$$M_n(R_{n,ta,a}) \subset \mathbb{A}\left(l(t) - \epsilon, u(t) + \epsilon\right).$$

Proof. Suppose $|a| \geq u(t) + \epsilon = \frac{2}{|t|^2} + \frac{1}{|t|} + \frac{2}{|t|^2}\sqrt{1+|t|} + \epsilon$. If we examine the modulus of the critical values we see that $|ta \pm 2\sqrt{a}| \geq |ta| - 2\sqrt{|a|} = |a|^{1/2}(|t||a|^{1/2} - 2) \geq (u(t) + \epsilon)^{1/2}(|t|(u(t)+\epsilon)^{1/2} - 2)$. Thus we have

$$|ta \pm 2\sqrt{a}| \geq |ta| - 2\sqrt{|a|} \geq \frac{2}{|t|} + 1 + \frac{2}{|t|}\sqrt{1+|t|} + \epsilon|t| - 2\sqrt{\frac{2}{|t|^2} + \frac{1}{|t|} + \frac{2}{|t|^2}\sqrt{1+|t|} + \epsilon}.$$

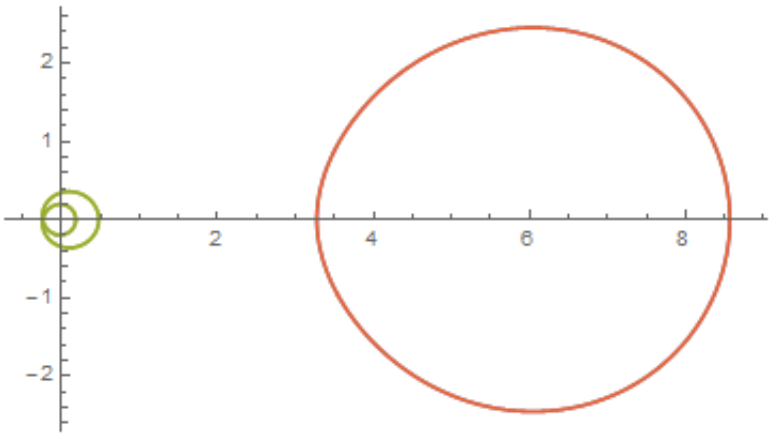

(a) Spine for $t = 0.8$

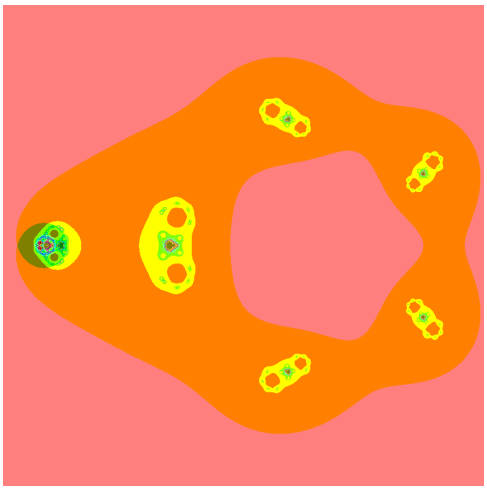

(b) Parameter plane slice for $t = 0.8$

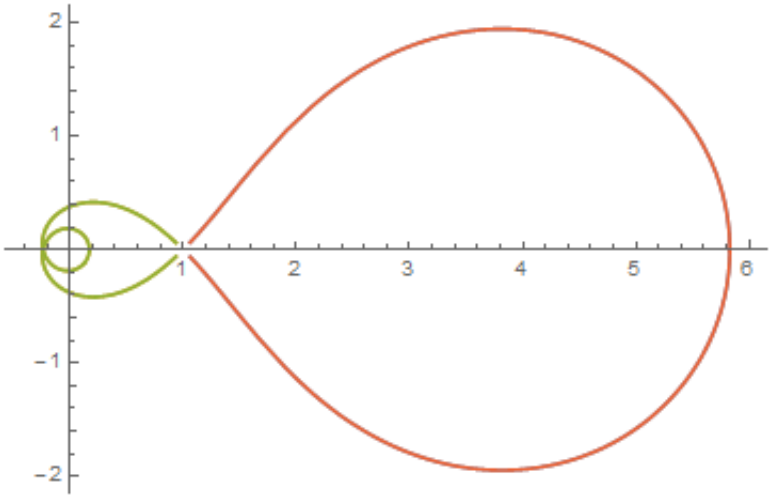

(c) Spine for $t = 1$

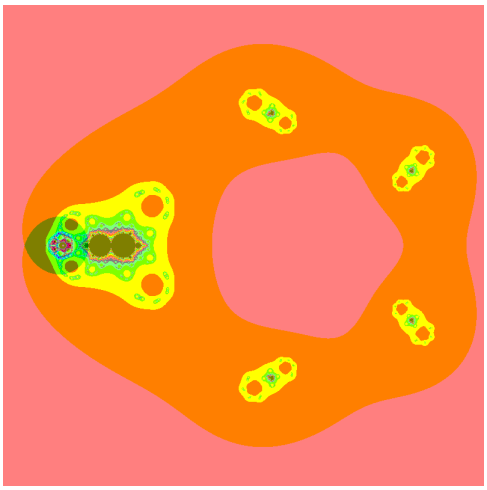

(d) Parameter plane slice for $t = 1$

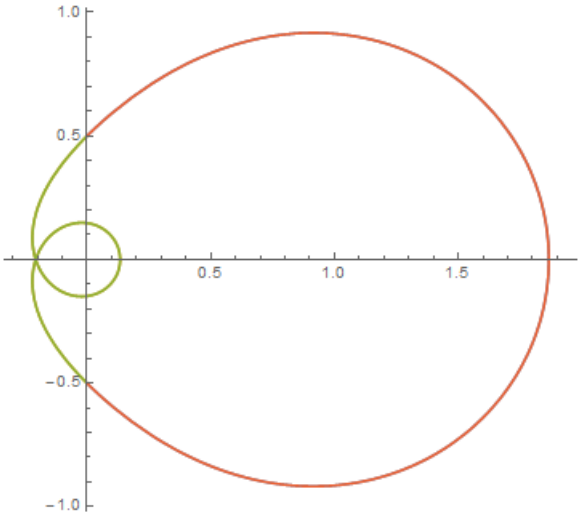

(e) Spine for $t = 2$

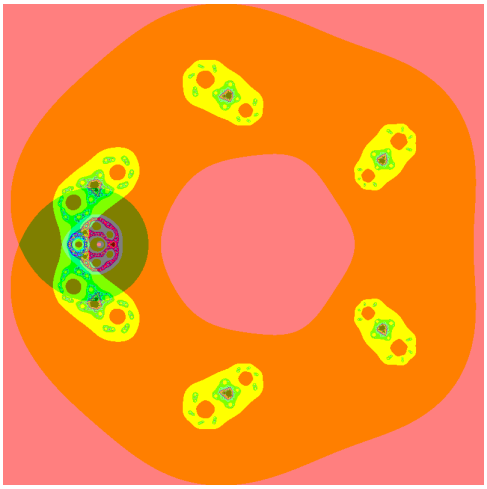

(f) Parameter plane slice for $t = 2$

Figure 5.3: Spines of $R_{5,ta,a}$

If we look at two terms from this last expression we notice that we can rewrite them

$$\begin{aligned}\frac{2}{|t|}+\frac{2}{|t|}\sqrt{1+|t|} &= \sqrt{\left(\frac{2}{|t|}+\frac{2}{|t|}\sqrt{1+|t|}\right)^2} \\ &= \sqrt{\frac{4}{|t|^2}+\frac{4}{|t|^2}(1+|t|)+\frac{8}{|t|^2}\sqrt{1+|t|}} \\ &= \sqrt{\frac{8}{|t|^2}+\frac{4}{|t|}+\frac{8}{|t|^2}\sqrt{1+|t|}} \\ &= 2\sqrt{\frac{2}{|t|^2}+\frac{1}{|t|}+\frac{2}{|t|^2}\sqrt{1+|t|}}.\end{aligned}$$

From this we get

$$\begin{aligned}|ta\pm 2\sqrt{a}| &\geq \frac{2}{|t|}+1+\frac{2}{|t|}\sqrt{1+|t|}+\epsilon|t|-2\sqrt{\frac{2}{|t|^2}+\frac{1}{|t|}+\frac{2}{|t|^2}\sqrt{1+|t|}+\epsilon} \\ &= 1+\epsilon|t|+\frac{2}{|t|}+\frac{2}{|t|}\sqrt{1+|t|}-2\sqrt{\frac{2}{|t|^2}+\frac{1}{|t|}+\frac{2}{|t|^2}\sqrt{1+|t|}+\epsilon} \\ &= 1+\epsilon|t|+2\sqrt{\frac{2}{|t|^2}+\frac{1}{|t|}+\frac{2}{|t|^2}\sqrt{1+|t|}}-2\sqrt{\frac{2}{|t|^2}+\frac{1}{|t|}+\frac{2}{|t|^2}\sqrt{1+|t|}+\epsilon}.\end{aligned}$$

For this argument we want to show that there exists some $\delta_1 > 0$ such that $|ta\pm 2\sqrt{a}| > 1+\delta_1$. In order to do this we must then show that

$$\epsilon|t|+2\sqrt{\frac{2}{|t|^2}+\frac{1}{|t|}+\frac{2}{|t|^2}\sqrt{1+|t|}}-2\sqrt{\frac{2}{|t|^2}+\frac{1}{|t|}+\frac{2}{|t|^2}\sqrt{1+|t|}+\epsilon} > 0.$$

If we fix any t and take the derivative of

$$\epsilon|t|+2\sqrt{\frac{2}{|t|^2}+\frac{1}{|t|}+\frac{2}{|t|^2}\sqrt{1+|t|}}-2\sqrt{\frac{2}{|t|^2}+\frac{1}{|t|}+\frac{2}{|t|^2}\sqrt{1+|t|}+\epsilon}$$

with respect to ϵ, we get

$$|t| - \frac{1}{\sqrt{\frac{2}{|t|^2} + \frac{1}{|t|} + \frac{2}{|t|^2}\sqrt{1+|t|} + \epsilon}}.$$

Next we look at where the derivative is positive:

$$\begin{aligned}
|t| - \frac{1}{\sqrt{\frac{2}{|t|^2} + \frac{1}{|t|} + \frac{2}{|t|^2}\sqrt{1+|t|} + \epsilon}} &> 0, \\
|t| &> \frac{1}{\sqrt{\frac{2}{|t|^2} + \frac{1}{|t|} + \frac{2}{|t|^2}\sqrt{1+|t|} + \epsilon}}, \\
|t|\sqrt{\frac{2}{|t|^2} + \frac{1}{|t|} + \frac{2}{|t|^2}\sqrt{1+|t|} + \epsilon} &> 1.
\end{aligned}$$

Since the left-hand side of this inequality is positive, we can square both sides to get

$$|t|^2\left(\frac{2}{|t|^2} + \frac{1}{|t|} + \frac{2}{|t|^2}\sqrt{1+|t|} + \epsilon\right) > 1,$$

or

$$2 + |t| + 2\sqrt{1+|t|} + \epsilon|t|^2 > 1.$$

Subtracting 1 from both sides gives us

$$1 + |t| + 2\sqrt{1+|t|} + \epsilon|t|^2 > 0,$$

which is true for any $\epsilon > 0$ and any choice of t. Therefore,

$$\epsilon|t| + 2\sqrt{\frac{2}{|t|^2} + \frac{1}{|t|} + \frac{2}{|t|^2}\sqrt{1+|t|}} - 2\sqrt{\frac{2}{|t|^2} + \frac{1}{|t|} + \frac{2}{|t|^2}\sqrt{1+|t|} + \epsilon}$$

is increasing with respect to ϵ. When $\epsilon = 0$,

$$\epsilon|t| + 2\sqrt{\frac{2}{|t|^2} + \frac{1}{|t|} + \frac{2}{|t|^2}\sqrt{1+|t|}} - 2\sqrt{\frac{2}{|t|^2} + \frac{1}{|t|} + \frac{2}{|t|^2}\sqrt{1+|t|} + \epsilon} = 0.$$

This, combined with the fact that it is increasing with respect to ϵ gives us that, whenever $\epsilon > 0$,

$$\epsilon|t| + 2\sqrt{\frac{2}{|t|^2} + \frac{1}{|t|} + \frac{2}{|t|^2}\sqrt{1+|t|}} - 2\sqrt{\frac{2}{|t|^2} + \frac{1}{|t|} + \frac{2}{|t|^2}\sqrt{1+|t|} + \epsilon} > 0.$$

Thus, there exists some $\delta_1 > 0$ such that

$$1 + \epsilon|t| + 2\sqrt{\frac{2}{|t|^2} + \frac{1}{|t|} + \frac{2}{|t|^2}\sqrt{1+|t|}} - 2\sqrt{\frac{2}{|t|^2} + \frac{1}{|t|} + \frac{2}{|t|^2}\sqrt{1+|t|} + \epsilon} > 1 + \delta_1,$$

and therefore

$$|ta \pm 2\sqrt{a}| > 1 + \delta_1.$$

By Corollary 2.4 this means that for any choice of a where $|a| \geq u(t) + \epsilon$ there exists an $N_1 \geq 2$ such that for all $n \geq N_1$ we have $ta \pm 2\sqrt{a} \notin K(R_{n,ta,a})$. Thus whenever $|a| \geq u(t) + \epsilon$ there exists an $N_1 \geq 2$ such that for all $n \geq N_1$ we get $a \notin M_n(R_{n,ta,a})$. Next we will use a similar process to show that we also have $a \notin M_n(R_{n,ta,a})$ for values of a which are within the hole at the center of the annulus.

Suppose $|a| \leq l(t) - \epsilon = \frac{2}{|t|^2} + \frac{1}{|t|} - \frac{2}{|t|^2}\sqrt{1+|t|} + \epsilon$. Just like above, we then have

$$\begin{aligned} |ta \pm 2\sqrt{a}| &\leq |ta| + 2\sqrt{|a|} \\ &\leq \frac{2}{|t|} + 1 - \frac{2}{|t|}\sqrt{1+|t|} - \epsilon|t| + 2\sqrt{\frac{2}{|t|^2} + \frac{1}{|t|} - \frac{2}{|t|^2}\sqrt{1+|t|} - \epsilon}. \end{aligned}$$

Again, looking at two terms from this expression, we can write

$$\begin{aligned}\frac{2}{|t|}-\frac{2}{|t|}\sqrt{1+|t|} &= -\sqrt{\left(\frac{2}{|t|}-\frac{2}{|t|}\sqrt{1+|t|}\right)^2} \\ &= -\sqrt{\frac{4}{|t|^2}+\frac{4}{|t|^2}(1+|t|)-\frac{8}{|t|^2}\sqrt{1+|t|}} \\ &= -\sqrt{\frac{8}{|t|^2}+\frac{4}{|t|}-\frac{8}{|t|^2}\sqrt{1+|t|}} \\ &= -2\sqrt{\frac{2}{|t|^2}+\frac{1}{|t|}-\frac{2}{|t|^2}\sqrt{1+|t|}}.\end{aligned}$$

Note that $\frac{2}{|t|}-\frac{2}{|t|}\sqrt{1+|t|}$ is negative, which is why we choose the negative square root above. Using this we can say

$$\begin{aligned}|ta\pm 2\sqrt{a}| &\leq \frac{2}{|t|}+1-\frac{2}{|t|}\sqrt{1+|t|}-\epsilon|t|+2\sqrt{\frac{2}{|t|^2}+\frac{1}{|t|}-\frac{2}{|t|^2}\sqrt{1+|t|}-\epsilon} \\ &= 1-\epsilon|t|+\frac{2}{|t|}-\frac{2}{|t|}\sqrt{1+|t|}+2\sqrt{\frac{2}{|t|^2}+\frac{1}{|t|}-\frac{2}{|t|^2}\sqrt{1+|t|}-\epsilon} \\ &= 1-\epsilon|t|-2\sqrt{\frac{2}{|t|^2}+\frac{1}{|t|}-\frac{2}{|t|^2}\sqrt{1+|t|}}+2\sqrt{\frac{2}{|t|^2}+\frac{1}{|t|}-\frac{2}{|t|^2}\sqrt{1+|t|}-\epsilon}.\end{aligned}$$

Notice that the two root terms in the final expression differ only by an epsilon under one of the roots. Thus the difference of these two roots is some small negative number with absolute value less than epsilon. This means that this final expression can be written as 1 minus $\epsilon|t|$ minus some small number. Thus there exists some $\delta_2 > 0$ such that we can write

$$|ta\pm 2\sqrt{a}| < 1-\delta_2.$$

By Corollary 2.4 this means that for any choice of a where $|a| \leq l(t)-\epsilon$ there exists an $N_2 \geq 2$ such that for all $n \geq N_2$ we have $ta\pm 2\sqrt{a} \notin K(R_{n,ta,a})$. Thus whenever $|a| \leq l(t)-\epsilon$ there exists an $N_2 \geq 2$ such that for all $n \geq N_2$ we get $a \notin M_n(R_{n,ta,a})$.

Finally, let $N = max(N_1, N_2)$ and we have our result; for all $n \geq N$ if $a \notin \mathbb{A}(l(t) - \epsilon, u(t) + \epsilon)$ then $a \notin M_n(R_{n,ta,a})$. $\square$

We now have an annulus in which the boundedness locus must lie. We could stop here but we would like to be a little more specific. The spine $\mathcal{S}_t$ lies inside this annulus but there is also plenty of wasted space inside this annulus which is not part of the boundedness locus. What we want to show is that the boundedness locus is within a neighborhood of $\mathcal{S}_t$ itself. This is a much more interesting result than finding a simple annulus which bounds the locus. In order to tackle the next Proposition we need to introduce a little notation.

Notation: We will denote the ϵ-neighborhood of a set S by $N_\epsilon(S)$, and the ball of radius ϵ centered at a point z by $B_\epsilon(z)$.

Theorem 5.3. *Let $\epsilon > 0$. There exists an $N \geq 2$ such that for all $n \geq N$ we have $M_n(R_{n,ta,a}) \subset N_\epsilon(\mathcal{S}_t)$.*

Proof. This proof follows the proof of Lemma 5.12 in [BS11] very closely. First, we apply Lemma 5.2 to get an N_1 such that for all $n \geq N_1$ we have $M_n(R_{n,ta,a}) \subset \mathbb{A}(l(t) - \epsilon, u(t) + \epsilon)$. Note that the proof of the lemma implies that $\mathcal{S}_t \subset \mathbb{A}(l(t), u(t))$. We want to show that if $a \notin N_\epsilon(\mathcal{S}_t)$ then $a \notin M_n(R_{n,ta,a})$, so there are two cases to consider.

First, if $a \notin \mathbb{A}(l(t) - \epsilon, u(t) + \epsilon)$, then by Lemma 5.2 we have $a \notin M_n(R_{n,ta,a})$.

Second, we must consider the set $H_{t,\epsilon} = \mathbb{A}(l(t) - \epsilon, u(t) + \epsilon) \setminus N_\epsilon(\mathcal{S}_t)$. This set is compact, so if we create an open cover of the set, $\{B_{\epsilon/2}(z) | z \in H_{t,\epsilon}\}$, it will have a finite subcover $\{B^1_{\epsilon/2}, B^2_{\epsilon/2}, ..., B^m_{\epsilon/2}\}$.

Since $0 \notin \mathbb{A}(l(t), u(t))$, we can take ϵ sufficiently small so that none of the $\{B^1_{\epsilon/2}, B^2_{\epsilon/2}, ..., B^m_{\epsilon/2}\}$ include 0. Therefore the square root function turns each $\{B^1_{\epsilon/2}, B^2_{\epsilon/2}, ..., B^m_{\epsilon/2}\}$ into two open neighborhoods, and $\left\{ta \pm 2\sqrt{B^k_{\epsilon/2}}\right\}$ is a collection of open neighborhoods with each $\overline{B^k_{\epsilon/2}} \subset \mathbb{C} \setminus N_{\epsilon/2}(\mathcal{S}_t)$. For each $B^k_{\epsilon/2}$ we can define a δ_k by

$$\delta_k = \min_{z \in \overline{B^k_{\epsilon/2}}} \left| \left| tz \pm 2\sqrt{z} \right| - 1 \right|.$$

From there we can define $\delta = \min_{1 \leq k \leq m} \delta_k$.

For this δ we can apply Corollary 2.4 to get an $N \geq N_1$ such that for all $n \geq N$ we have $K(R_{n,ta,a}) \subset N_\delta(S^1)$. However, for each $a \in H_{t,\epsilon}$ we also have a in one of the $B^k_{\epsilon/2}$, and therefore $||ta \pm 2\sqrt{a}| - 1| > \delta$. This means that both $ta \pm 2\sqrt{a} \notin K(R_{n,ta,a})$ and therefore $a \notin M_n(R_{n,ta,a})$.

Thus we have that, for all $n \geq N$, if $a \notin N_\epsilon(\mathcal{S}_t)$ then $a \notin M_n(R_{n,ta,a})$. Therefore $M_n(R_{n,ta,a}) \subset N_\epsilon(\mathcal{S}_t)$. $\square$

Chapter 6

Investigating a Family with One Critical Value a Fixed Point of $R_{n,c,a}$

In the last chapter we examined what happened when we asked: What happens when we allow two parameters to vary rather than just one? We set the parameter c so that two separate elements of the family of functions would vary as the a parameter varied. This allowed us to look at a collection of different one-dimensional slices of (c, a), in which we still saw baby Mandelbrot sets. In this chapter we examine a dynamically significant one-dimensional slice through (c, a). Specifically, we examine a set of parameter values for which one critical value is a fixed point for the map. We will explore this idea by once more reparameterizing our original family of complex rational functions. This time we will set c so that $c+2\sqrt{a} = a^{1/2n}$ is always true for the canonical choice of roots for $a^{1/2n}$. Specifically, if $arg(a) = \psi$, then $c = |a|^{1/2n}e^{i\frac{\psi}{2n}} - 2\sqrt{a}$. For the most part, however, we will simply refer to c as $c = a^{1/2n} - 2\sqrt{a}$. This distinction will come into play only when we try to find values of a for which one of the critical points $a^{1/2n}$ maps to the other critical value, $c - 2\sqrt{a}$. To be precise, let $f_n(a) = a^{1/2n} - 2\sqrt{a}$. We will be looking at the behavior of the family of functions

$$R_{n,f(a),a}(z) = z^n + \frac{a}{z^n} + a^{1/2n} - 2\sqrt{a},$$

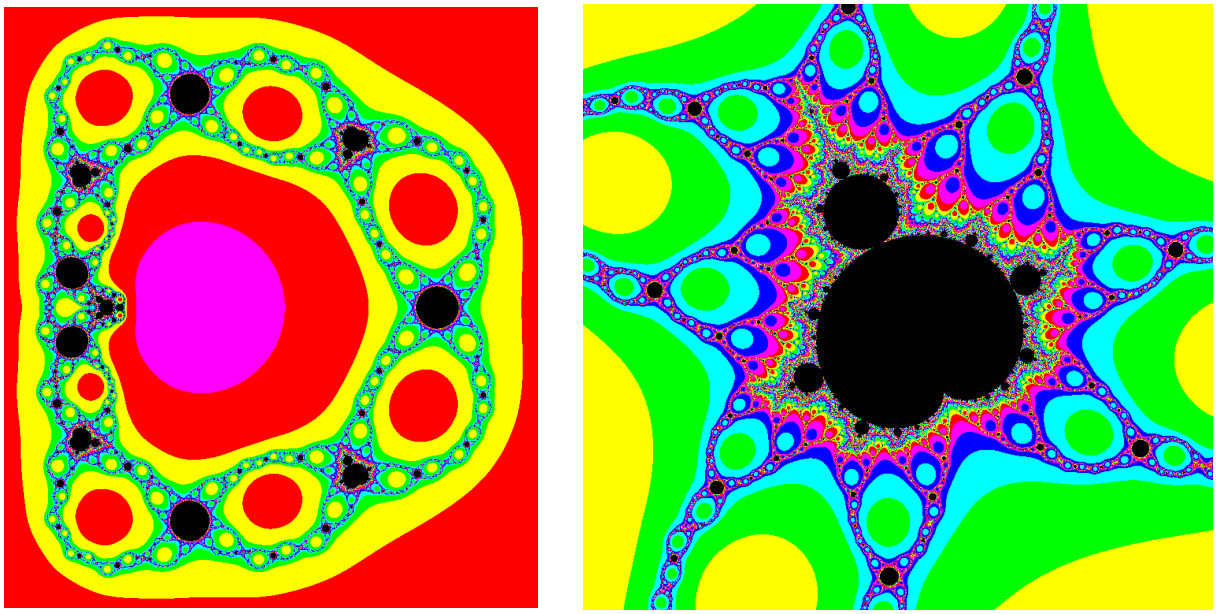

(a) Parameter plane for $n = 6$

(b) Zoomed in on 'Mandelbrot' set

Figure 6.1: The parameter slice for $R_{6,a}$

where $n \geq 3$ and $a \in \mathbb{C} \setminus \{0\}$. For simplicity's sake, we will refer to this parameterization as $R_{n,a}$ for the rest of the chapter.

Figure 6.1 shows an example of one a-plane for this family. The first thing that stands out are the brighter colors in comparison to previous pictures. One of the critical orbits is fixed, and so is always bounded. This means there is only one free critical orbit to track, so we get bright, crisp images which aren't darkened by two competing color schemes. Once again we see possible baby Mandelbrot sets showing up in the parameter plane. We also see small black disks throughout the boundedness locus. As we increase n we see some interesting patterns emerge. Figure 6.2 shows multiple a-parameter planes to illustrate this. There are what look like $n-2$ well-defined baby Mandelbrot sets in each plane, as well as $n-1$ large filled disks. There also appear to be more disks and Mandelbrot sets throughout the necklace structure in these images, but these $n-1$ disks and $n-2$ 'Mandelbrot sets' are the most prominent. Lastly, there is also a shape present in each which almost looks like two Mandelbrot sets mashed together. What we would like to do is to identify a curve near which this behavior is occurring, and then to try to explain why these shapes occur.

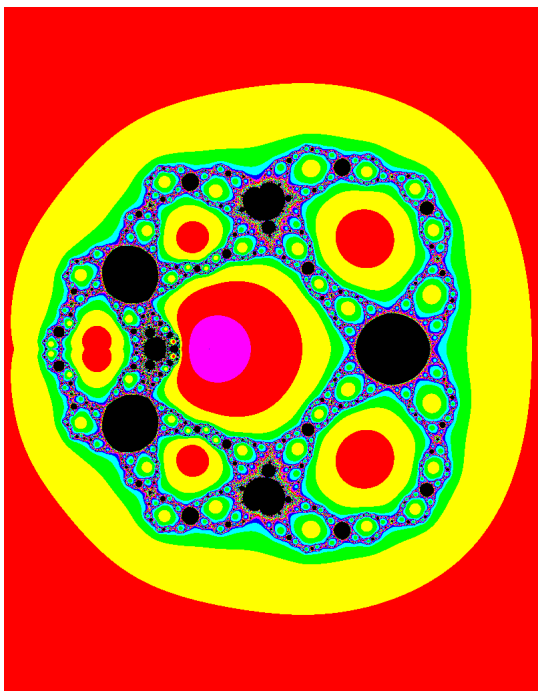

(a) Parameter plane for $n = 4$

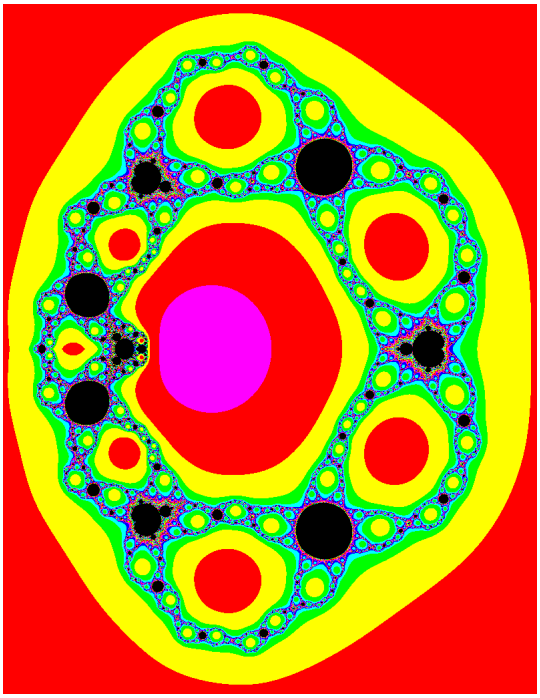

(b) Parameter plane for $n = 5$

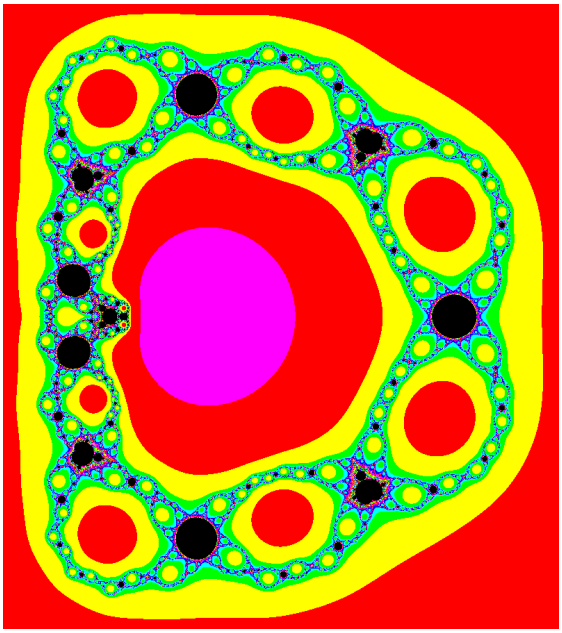

(c) Parameter plane for $n = 6$

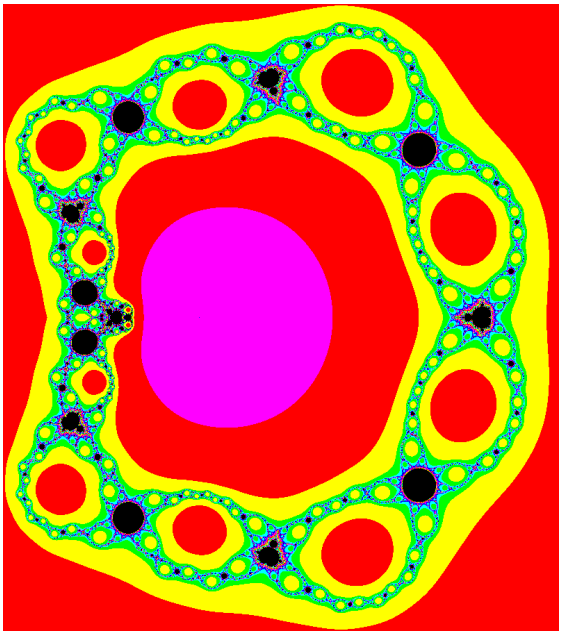

(d) Parameter plane for $n = 7$

Figure 6.2: Parameter planes for $R_{n,a}$ for $n = 4$, 5, 6, and 7

6.1 The Spines of $R_{n,a}$

In the previous chapter we were able to describe the region in which the boundedness locus of $R_{n,ta,a}$ must lie. We did this by first finding a curve consisting of a-values which are solutions

to one of the equations $c \pm 2\sqrt{a} = 1$, and then extending an epsilon neighborhood around this curve. For $R_{n,a}$ the same argument can not be used to find a region for the boundedness locus. However, we are still able to find a spine for $R_{n,a}$. Just as in the last chapter, we do so by examining the values of a for which the bounded critical orbits lie on the unit circle.

Proposition 6.1. *For $c = a^{1/2n} - 2\sqrt{a}$, the set of all $a \in \mathbb{C}$ for which at least one of the equations $|c \pm 2\sqrt{a}| = 1$ holds true is given by the solutions to*

$$a = \frac{1}{16}(a^{1/2n} + e^{i\theta})^2 \quad \textit{for} \quad 0 \leq \theta \leq 2\pi.$$

As n gets large, this is very close to the cardioid

$$a = \frac{1}{16}(1 + e^{i\theta})^2 \quad \textit{for} \quad 0 \leq \theta \leq 2\pi,$$

which has a cusp at 0 on the left side of the figure.

Proof. We first write $|c \pm 2\sqrt{a}| = 1$ as $c \pm 2\sqrt{a} = -e^{i\theta}$ for $0 \leq \theta \leq 2\pi$. Substituting $c = a^{1/2n} - 2\sqrt{a}$ gives us two equations to consider:

$$a^{1/2n} = -e^{i\theta},$$

and

$$a^{1/2n} - 4\sqrt{a} = -e^{i\theta}.$$

The first equation represents the critical value $c + 2\sqrt{a}$, which we know is fixed and so will only lie near the unit circle when $|a| = 1$. As for the second equation, we will get the form that we are looking for by isolating the square root term and then solving for that a.

$$a^{1/2n} - 4\sqrt{a} = -e^{i\theta},$$

so

$$\begin{aligned} 4\sqrt{a} &= a^{1/2n} + e^{i\theta}, \\ \sqrt{a} &= \frac{1}{4}(a^{1/2n} + e^{i\theta}), \\ a &= \frac{1}{16}(a^{1/2n} + e^{i\theta})^2. \end{aligned}$$

□

It may not be obvious from Figure 6.2 that this spine becomes more and more like a cardioid as n gets larger. If we trace the large black shapes within the necklace structure we can see a curve which looks at least somewhat like a cardioid as early as $n = 6$. Figure 6.3 shows an example of a large value of n where we very clearly see a cardioid shape.

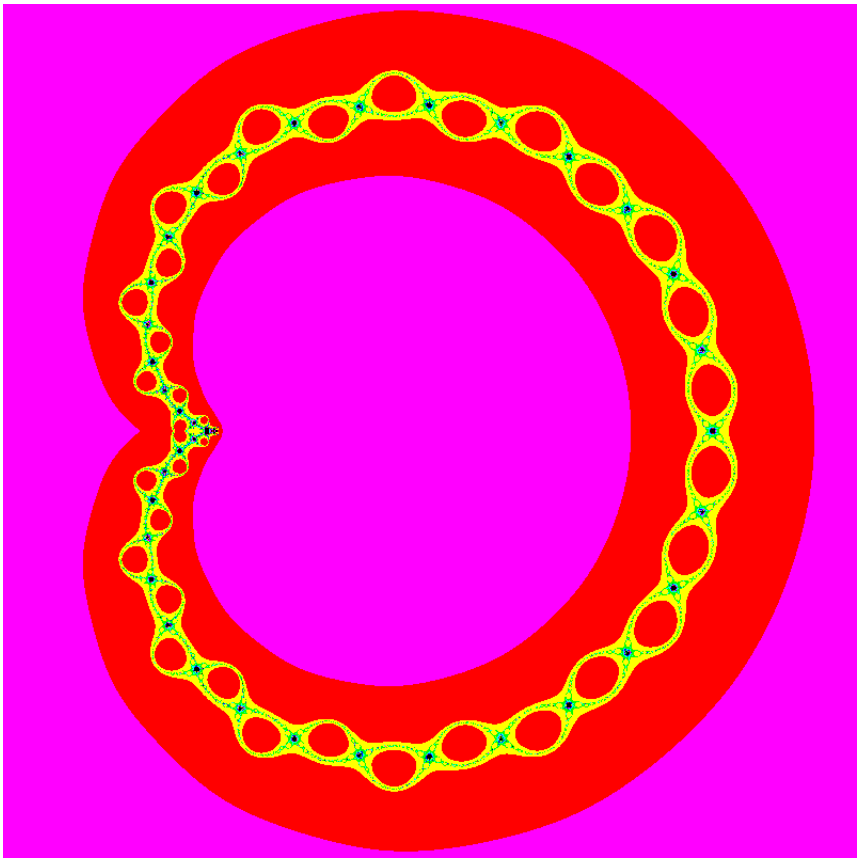

Figure 6.3: Parameter plane for $n = 20$

6.2 Centers of Baby Mandelbrot Sets

With earlier families of complex rational functions that we examined baby Mandelbrot sets tend to spring up around values of the parameter a for which one of the critical values is fixed. With $R_{n,a}$, however, the critical value $c + 2\sqrt{a}$ is always fixed. Therefore any interesting behavior should happen near values of a for which the second critical value, $c - 2\sqrt{a}$, is fixed as well. This should allow us to find the locations of the observed disks and baby Mandelbrot sets, and hopefully even allow us to differentiate between which a-values produce which shape.

Fixing $c - 2\sqrt{a}$ means we have $c - 2\sqrt{a} = a^{1/2n}$ for one of the $2n^{\text{th}}$ roots of a. The critical value $c + 2\sqrt{a}$ is set equal to $|a|^{\frac{1}{2n}} e^{\frac{\psi}{2n}}$, which we will call the canonical $2n^{\text{th}}$ root of a. This gives us one trivial solution: If $a = 0$, then $c - 2\sqrt{a} = c + 2\sqrt{a} = a^{1/2n} = 0$. For the rest we need $c - 2\sqrt{a}$ to be equal to a non-canonical choice of root, so a little more work is required.

Proposition 6.2. *The set of a-values for which the critical value $c - 2\sqrt{a}$ is equal to one of the non-canonical roots of $a^{1/2n}$ is given by*

$$a = \left(\frac{1 - e^{i\frac{k\pi}{n}}}{4} \right)^{\frac{2n}{n-1}} \quad \textit{for} \quad k = 1, 2, 3, ..., 2n - 1.$$

Proof. Here we are taking the critical value $c - 2\sqrt{a}$ and setting it equal to $a^{1/2n}$. This gives us

$$c - 2\sqrt{a} = a^{1/2n},$$

or

$$a^{1/2n} - 4\sqrt{a} = a^{1/2n}.$$

The important thing to note here is that when we are substituting $a^{1/2n} - 2\sqrt{a}$ in for c, we are using the canonical choice for the root $a^{1/2n}$. In order to avoid a trivial equation, the $a^{1/2n}$ root on the right-hand side of the equation must **not** be the same canonical root. It must be chosen from one of the $2n - 1$ other roots. Thus we really have $2n - 1$ equations to

consider, all of the following form:

$$a^{1/2n} - 4\sqrt{a} = a^{1/2n} e^{i\frac{k\pi}{n}} \quad \text{for} \quad k = 1, 2, 3, ..., 2n-1.$$

We rearrange the equation to first isolate the square root term, then solve for a:

$$\begin{aligned}
4\sqrt{a} &= a^{1/2n} - a^{1/2n} e^{i\frac{k\pi}{n}}, \\
\sqrt{a} &= \frac{a^{1/2n} - a^{1/2n} e^{i\frac{k\pi}{n}}}{4}, \\
\sqrt{a} &= a^{1/2n} \left(\frac{1 - e^{i\frac{k\pi}{n}}}{4} \right), \\
a^{\frac{n-1}{2n}} &= \frac{1 - e^{i\frac{k\pi}{n}}}{4}, \\
a &= \left(\frac{1 - e^{i\frac{k\pi}{n}}}{4} \right)^{\frac{2n}{n-1}}.
\end{aligned}$$

Thus we have

$$a = \left(\frac{1 - e^{i\frac{k\pi}{n}}}{4} \right)^{\frac{2n}{n-1}} \quad \text{for} \quad k = 1, 2, 3, ..., 2n-1.$$

□

At each of these $2n-1$ points we see some interesting behavior. Some of them lie within observed baby Mandelbrot sets and some of them are inside the filled disks we see in the boundedness locus. We would like to be able to predict if particular points in this collection correspond to particular types of shapes. To this end, we can get some more information about this collection of points by examining the images of the critical value $c - 2\sqrt{a}$ under $R_{n,a}(z)$ at the $2n-1$ a-values listed above. When we do so, two patterns emerge.

Theorem 6.3. *Let*

$$a = \left(\frac{1 - e^{i\frac{k\pi}{n}}}{4} \right)^{\frac{2n}{n-1}} \quad \textit{for} \quad k = 1, 2, 3, ..., 2n-1,$$

and define $c = a^{1/2n} - 2\sqrt{a}$. *Then for each* $k = 1, 2, 3, ..., 2n-1$, *if* k *is odd then the critical value* $c - 2\sqrt{a}$ *is fixed at a non-canonical root of* $a^{1/2n}$. *If* k *is even, then* $c - 2\sqrt{a}$ *maps to* $c + 2\sqrt{a}$.

Proof. Let $a = \left(\frac{1-e^{i\frac{k\pi}{n}}}{4}\right)^{\frac{2n}{n-1}}$ and $c = a^{1/2n} - 2\sqrt{a}$. Before substituting these values into the function we will first simplify things a bit. We want to show that

$$R_{n,a}(c - 2\sqrt{a}) = (c - 2\sqrt{a})^n + \frac{a}{(c - 2\sqrt{a})^n} + c = c \pm 2\sqrt{a}.$$

To make the equations a bit less messy we will subtract a c from both sides. Thus we will instead show that

$$(c - 2\sqrt{a})^n + \frac{a}{(c - 2\sqrt{a})^n} = \pm 2\sqrt{a}.$$

Plugging $c = a^{1/2n} - 2\sqrt{a}$ and $a = \left(\frac{1-e^{i\frac{k\pi}{n}}}{4}\right)^{\frac{2n}{n-1}}$ into $(c - 2\sqrt{a})^n + \frac{a}{(c-2\sqrt{a})^n}$ we get

$$\left(\left(\frac{1 - e^{i\frac{k\pi}{n}}}{4}\right)^{\frac{1}{n-1}} - 4\left(\frac{1 - e^{i\frac{k\pi}{n}}}{4}\right)^{\frac{n}{n-1}}\right)^n + \frac{\left(\frac{1-e^{i\frac{k\pi}{n}}}{4}\right)^{\frac{2n}{n-1}}}{\left(\left(\frac{1-e^{i\frac{k\pi}{n}}}{4}\right)^{\frac{1}{n-1}} - 4\left(\frac{1-e^{i\frac{k\pi}{n}}}{4}\right)^{\frac{n}{n-1}}\right)^n}.$$

Next we factor $\left(\frac{1-e^{i\frac{k\pi}{n}}}{4}\right)^{\frac{n}{n-1}}$ out of both of these terms, which gives us

$$\left(\frac{\left(\left(\frac{1-e^{i\frac{k\pi}{n}}}{4}\right)^{\frac{1}{n-1}} - 4\left(\frac{1-e^{i\frac{k\pi}{n}}}{4}\right)^{\frac{n}{n-1}}\right)^n}{\left(\frac{1-e^{i\frac{k\pi}{n}}}{4}\right)^{\frac{n}{n-1}}} + \frac{\left(\frac{1-e^{i\frac{k\pi}{n}}}{4}\right)^{\frac{n}{n-1}}}{\left(\left(\frac{1-e^{i\frac{k\pi}{n}}}{4}\right)^{\frac{1}{n-1}} - 4\left(\frac{1-e^{i\frac{k\pi}{n}}}{4}\right)^{\frac{n}{n-1}}\right)^n}\right)\left(\frac{1 - e^{i\frac{k\pi}{n}}}{4}\right)^{\frac{n}{n-1}}.$$

From here we can bring the numerator and denominator of each of these large fractions under the same exponent:

$$\left(\left(\frac{\left(\frac{1-e^{i\frac{k\pi}{n}}}{4}\right)^{\frac{1}{n-1}}-4\left(\frac{1-e^{i\frac{k\pi}{n}}}{4}\right)^{\frac{n}{n-1}}}{\left(\frac{1-e^{i\frac{k\pi}{n}}}{4}\right)^{\frac{1}{n-1}}}\right)^{n}+\left(\frac{\left(\frac{1-e^{i\frac{k\pi}{n}}}{4}\right)^{\frac{1}{n-1}}}{\left(\frac{1-e^{i\frac{k\pi}{n}}}{4}\right)^{\frac{1}{n-1}}-4\left(\frac{1-e^{i\frac{k\pi}{n}}}{4}\right)^{\frac{n}{n-1}}}\right)^{n}\right)\left(\frac{1-e^{i\frac{k\pi}{n}}}{4}\right)^{\frac{n}{n-1}}.$$

We get some cancellation in each large fraction, so the expression simplifies to

$$\left(\left(1-4\left(\frac{1-e^{i\frac{k\pi}{n}}}{4}\right)^{\frac{n-1}{n-1}}\right)^{n}+\left(\frac{1}{1-4\left(\frac{1-e^{i\frac{k\pi}{n}}}{4}\right)^{\frac{n-1}{n-1}}}\right)^{n}\right)\left(\frac{1-e^{i\frac{k\pi}{n}}}{4}\right)^{\frac{n}{n-1}}.$$

Simplifying further leaves us with

$$\left(e^{ik\pi}+e^{-ik\pi}\right)\left(\frac{1-e^{i\frac{k\pi}{n}}}{4}\right)^{\frac{n}{n-1}}.$$

Since $a=\left(\frac{1-e^{i\frac{k\pi}{n}}}{4}\right)^{\frac{2n}{n-1}}$, we can write this as

$$\left(e^{ik\pi}+e^{-ik\pi}\right)\sqrt{a}.$$

It is now easy to see that if k is odd this expression is equal to $-2\sqrt{a}$ and if k is even it is equal to $2\sqrt{a}$. Thus, if k is odd then

$$R_{n,c}(c-2\sqrt{a})=c-2\sqrt{a}$$

and if k is even then

$$R_{n,c}(c-2\sqrt{a})=c+2\sqrt{a}.$$

□

Chapter 7

Future Work

In this chapter we'll briefly discuss a few avenues for future work on this subject. They all revolve around the identification of one of two types of shapes that appear within the (c, a) space of this family of functions $R_{n,c,a}$.

7.1 Baby Julia Sets

Throughout almost all of the images presented in this paper it becomes almost immediately clear that there are Mandelbrot-like shapes present in these slices of the (c, a) parameter space that we have studied. What is not readily apparent is that in many cases there are also smaller shapes, often buried in the necklace structure surrounding the Mandelbrot sets, which resemble quadratic Julia sets. They seem to arise in situations where both critical orbits have varying behavior. In the a-parameter plane for fixed n and c they appear when the two necklace structures representing each of the two critical orbits overlap. Figure 7.1 shows a very close zoom of part of the necklace structure of $R_{n,c,a}$ for $n = 8$ and $c = 0.08$ next to the filled Julia set for P_c with $c = 0.1 - 0.45i$. We can also see these quadratic Julia sets in the necklace structure of some of the other slices that we looked at. Figure 7.2a shows a shape appearing in the necklace structure of $R_{n,ta,a}$ for $n = 4$ and $t = 6$, while Figure 7.2b shows the filled Julia set of P_c for $c = -1.3 + 0.02i$.

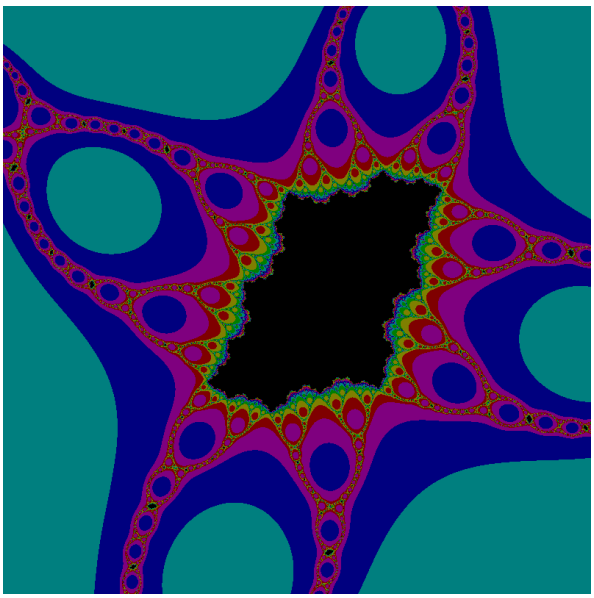

(a) Figure in the necklace of $R_{8,0.08,a}$

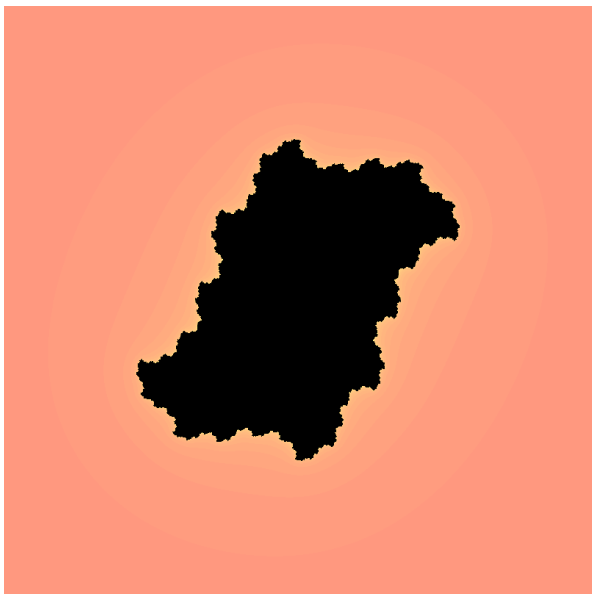

(b) Filled Julia set for P_c with $c = 0.1 - 0.45i$

Figure 7.1: Shape appearing in the a-plane of $R_{n,c,a}$ versus a quadratic filled Julia set

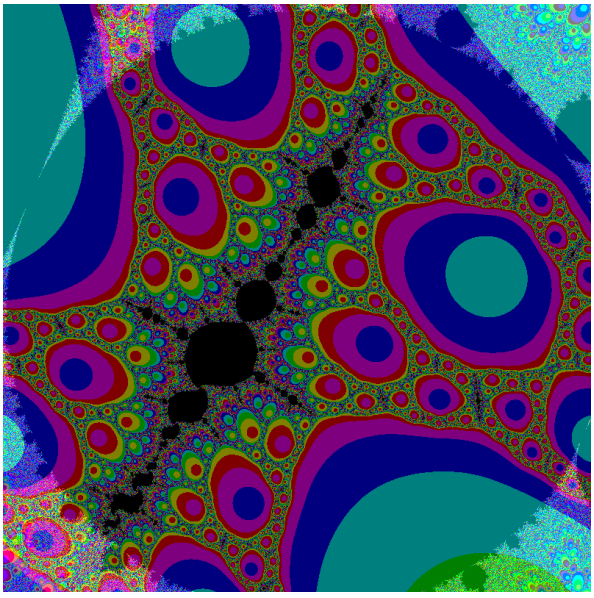

(a) Figure in the necklace of $R_{4,6a,a}$

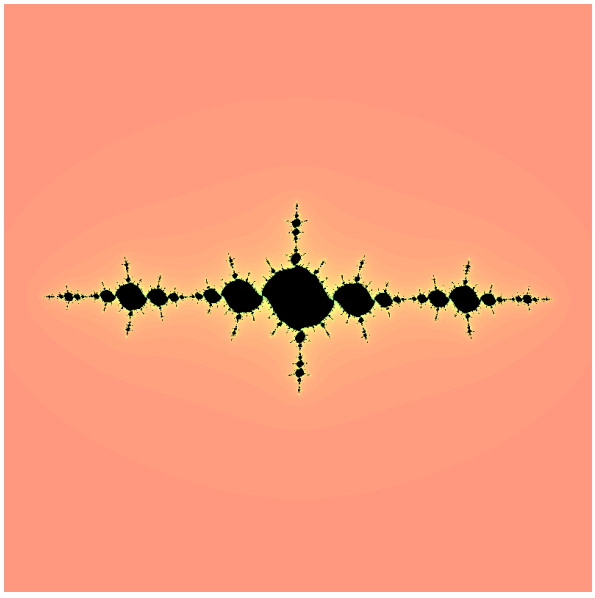

(b) Filled Julia set for P_c with $c = -1.3 + 0.02i$

Figure 7.2: Comparison of a shape in the parameter plane of $R_{n,ta,a}$ and a Julia set

In both cases we see what look like quadratic Julia sets appearing within various parameter planes of the family of complex functions. We did some work in Chapter 4 showing that baby quadratic Julia sets appear within the filled Julia sets of $R_{n,c,a}$, but we have not yet explored these occurrences in the boundedness loci. This leads us to an avenue of study which would be similar to the work done in this paper, but which would likely require the use of tools other than what have been developed here.

Conjecture 1. *There exist homeomorphic copies of Julia sets of P_c within the boundedness loci of the parameter planes of $R_{n,c,a}$.*

7.2 Baby Mandelbrot Sets

A natural continuation of the work done in this paper would involve returning to the slices of the (c, a) space which were discussed in chapters 5 and 6. With both $R_{n,ta,a}$ and $R_{n,a}$ we have yet to prove the existence of homeomorphic copies of the Mandelbrot set within the parameter planes.

7.2.1 $R_{n,ta,a}$

For $R_{n,ta,a}$ we identified both a spine around which the boundedness locus must be centered. We also determined a region around this spine in which the boundedness locus must lie. The next steps would be to find centers for where the baby Mandelbrot sets should be, and then to prove explicitly that they are present.

Conjecture 2. *There exist homeomorphic copies of the Mandelbrot set within the one-complex dimensional slices of the (c, a) space of the parameterization of $R_{n,c,a}$ given by $c = ta$.*

7.2.2 $R_{n,a}$

In Chapter 6 we saw an interesting parameterization where both baby Mandelbrot sets and filled disks appeared to be present in the parameter planes. We were able to find a spine for

this parameterization, as well as a collection of $2n-1$ a-values at which $c-2\sqrt{a}$ lands on a non-canonical critical point. These values could be separated into two groups: n values at which $c-2\sqrt{a}$ remains fixed, and $n-1$ values at which $c-2\sqrt{a}$ maps to $c+2\sqrt{a}$.

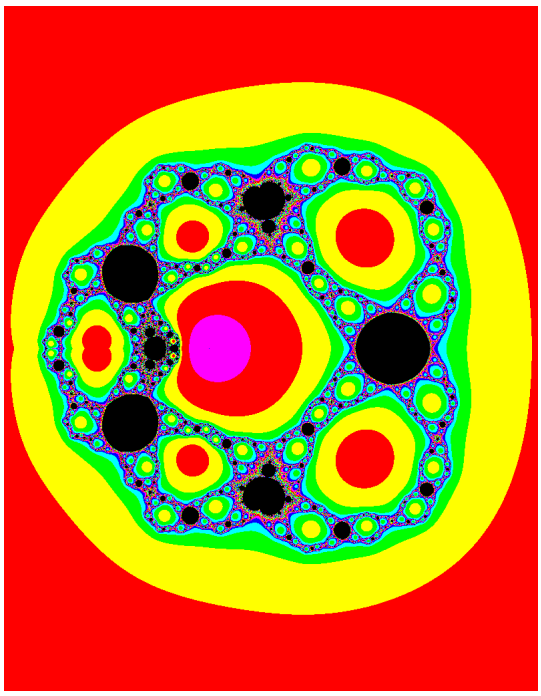

(a) Parameter plane for $n=4$

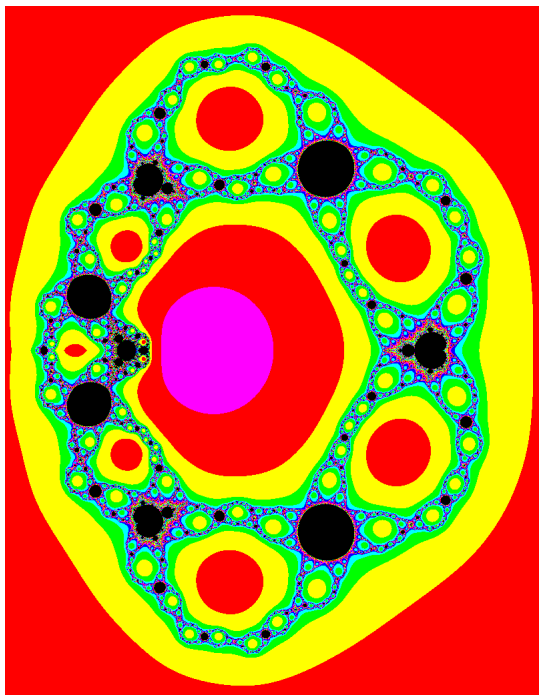

(b) Parameter plane for $n=5$

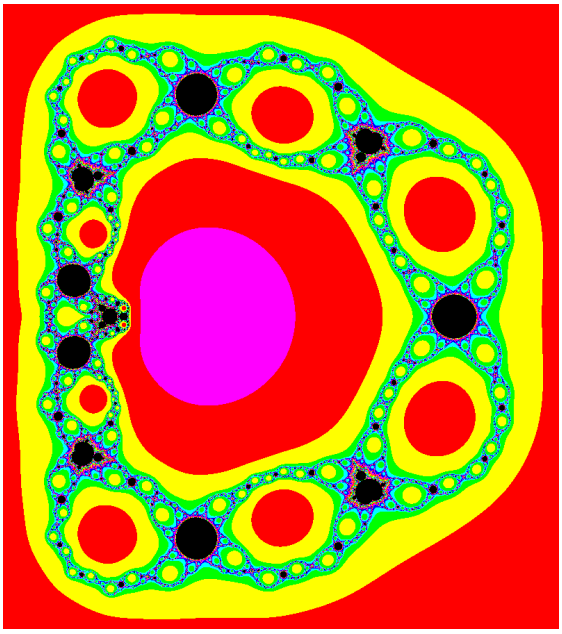

(c) Parameter plane for $n=6$

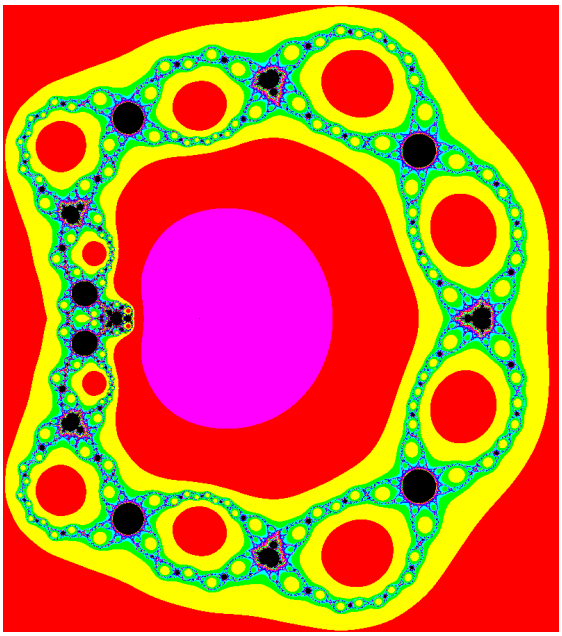

(d) Parameter plane for $n=7$

Figure 7.3: Parameter planes for $R_{n,a}$ for $n=4$, 5, 6, and 7

If we examine the images for this parameterization, we see what look like $n-2$ baby Mandelbrot sets, $n-1$ solid disks, and a shape near 0 which looks a bit like two Mandelbrot sets mashed together.

I would posit that each apparent baby Mandelbrot set should correspond to one of the n values at which $c-2\sqrt{a}$ remains fixed, with the remaining two landing inside the 'mashed' figure nearest the center. These a-values are those at which the behavior of $c-2\sqrt{a}$ is fixed, but in a different way than that of $c+2\sqrt{a}$. For this reason each of these a-values should correspond to a baby Mandelbrot set. Two of them, however, remain to close to each other and so the baby Mandelbrot sets overlap and distort.

The $n-1$ remaining a-values, at which $c-2\sqrt{a}$ maps to $c+2\sqrt{a}$, should correspond to the centers of the filled disks that are present in the images. At these values the two critical orbits become identical. If we could show that these are homeomorphic to quadratic Julia sets, it would serve to show even further that the local behavior of the critical orbits of these families of functions is similar to the dynamics of a polynomial. Similar work has been done [BH01, Mit16], so I believe that is it something that can be approached.

Conjecture 3. *There exist homeomorphic copies of the Mandelbrot set within the parameter planes of the family of functions* $R_{n,a}(z) = z^n + \frac{a}{z^n} + a^{1/2n} - 2\sqrt{a}$. *There also exist homeomorphic copies of the filled Julia set of* $P_0 = z^2$ *within the parameter planes of* $R_{n,a}$.

Yet one more possible direction would be to investigate behavior when one critical orbit is prescribed in a more complicated way. For example, if we set one critical orbit so that it is always in a two-cycle, would we see baby basilicas (quadratic Julia sets which appear when the critical orbit falls into a two-cycle) in the parameter space rather than the disks that we saw here in Chapter 6? Fixing the behavior of one critical orbit opens up many interesting options to look into. Our work in Chapter 6 produced some of the more striking images, so it would be very interesting to see what other pattern could emerge.

Bibliography

[BB] Brian Boyd and Suzanne Boyd. Dynamics Explorer, at sourceforge. [http://sourceforge.net/projects/detool].

[BDGR08] Paul Blanchard, Robert L. Devaney, Antonio Garijo, and Elizabeth D. Russell. A generalized version of the McMullen domain. *Internat. J. Bifur. Chaos Appl. Sci. Engrg.*, 18(8):2309–2318, 2008.

[Bea91] Alan F. Beardon. *Iteration of Rational Functions*, volume 132 of *Graduate Texts in Mathematics*. Springer-Verlag, New York, 1991. Complex analytic dynamical systems.

[BH01] X. Buff and C. Henriksen. Julia sets in parameter spaces. *Comm. Math. Phys.*, 220(2):333–375, 2001.

[BS11] Suzanne Boyd and Michael Schulz. Geometric limits of Mandelbrot and Julia sets under degree growth. *ArXiv e-prints*, 1109.2166v1, September 2011.

[DBC+13] Robert L. Devaney, Paul Blanchard, Figen Cilingir, Daniel Cuzzocreo, Daniel M. Look, and Elizabeth D. Russell. Checkerboard Julia Sets for Rational Maps. *Int'l Bifurcation and Chaos*, 23:48–60, 2013.

[DBC+14] Robert L. Devaney, Paul Blanchard, Daniel Cuzzocreo, Elizabeth Fitzgibbon, and Stefano Silvestri. A Dynamical Invariant for Sierpinski Cardioid Julia Sets. *Fundamenta Mathematicae*, 226:253–277, 2014.

[DBCF16] Robert L. Devaney, Paul Blanchard, Daniel Cuzzocreo, and Elizabeth Fitzgibbon. Accessible Mandelbrot Sets in the Family $z^n + \frac{\lambda}{z^n}$. *Qualitative Theory of Dynamical Systems*, 15:49–66, 2016.

[Dev06] Robert L. Devaney. Baby Mandelbrot sets adorned with halos in families of rational maps. In *Complex dynamics*, volume 396 of *Contemp. Math.*, pages 37–50. Amer. Math. Soc., Providence, RI, 2006.

[Dev09] Robert L. Devaney. Intertwined Internal Rays in Julia Sets of Rational Maps. *Fundamenta Mathematicae*, 206:139–159, 2009.

[Dev12] Robert L. Devaney. Dynamics of $z^n + \frac{\lambda}{z^n}$; Why the Case $n = 2$ is Crazy. In *Conformal Dynamics and Hyperbolic Geometry*, volume 573 of *Contemp. Math.*, pages 49–65. Amer. Math. Soc., Providence, RI, 2012.

[Dev13] Robert L. Devaney. Singular perturbations of complex polynomials. *Bull. Amer. Math. Soc. (N.S.)*, 50(3):391–429, 2013.

[Dev14] Robert L. Devaney. Limiting Behavior of Julia Sets of Singularly Perturbed Rational Maps. In *Frontiers in Complex Dynamics: In Celebration of John Milnor's 80th Birthday*, pages 121–134. Princeton University Press, 2014.

[DH85] Adrien Douady and John Hamal Hubbard. On the dynamics of polynomial-like mappings. *Ann. Sci. École Norm. Sup. (4)*, 18(2):287–343, 1985.

[DR13] Robert L. Devaney and Elizabeth D. Russell. Connectivity of Julia Sets for Singularly Perturbed Rational Maps. In *Chaos, CNN, Memristors and Beyond*, pages 239–245. World Scientific, 2013.

[GC93] Theodore W. Gamelin and Lennart Carleson. *Complex Dynamics*. Springer-Verlag, New York, 1993.

[KD14] Robert T. Kozma and Robert L. Devaney. Julia sets converging to filled quadratic Julia sets. *Ergodic Theory Dynam. Systems*, 34(1):171–184, 2014.

[Mit16] Alexander Mitchell. *Existence of the Mandelbrot Set in the Parameter Planes of Certain Rational Functions*. PhD thesis, University of Wisconsin - Milwaukee, 2016.

[Roe06] P. Roesch. On capture zones for the family $f_\lambda(z) = z^2 + \lambda/z^2$. In *Dynamics on the Riemann sphere*, pages 121–129. Eur. Math. Soc., Zürich, 2006.

[Shi87] Mitsuhiro Shishikura. On the quasiconformal surgery of rational functions. *Ann. Sci. École Norm. Sup. (4)*, 20(1):1–29, 1987.

CURRICULUM VITAE

Matthew Hoeppner

Place of birth: Tuscaloosa, AL

Education

B.A., Mathematics, Kalamazoo College, May 2007

M.S., Mathematics, University of Wisconsin – Milwaukee, May 2012

Ph.D., Mathematics, University of Wisconsin – Milwaukee, May 2017

Dissertation Title: On Some One-Complex Dimensional Slices of the Boundedness Locus of a Multi-Parameter Rational Family.